

On the Convergence of the Gradient Descent Method with Stochastic Fixed-point Rounding Errors under the Polyak–Łojasiewicz Inequality *

Lu Xia

Michiel E. Hochstenbach

*Department of Mathematics and Computer Science
Eindhoven University of Technology
Eindhoven, 5600 MB, The Netherlands*

L.XIA1@TUE.NL

M.E.HOCHSTENBACH@TUE.NL

Stefano Massei

*Department of Mathematics
Università di Pisa
Pisa, 56127, Italy*

STEFANO.MASSEI@UNIFI.IT

Abstract

When training neural networks with low-precision computation, rounding errors often cause stagnation or are detrimental to the convergence of the optimizers; in this paper we study the influence of rounding errors on the convergence of the gradient descent method for problems satisfying the Polyak–Łojasiewicz inequality. Within this context, we show that, in contrast, biased stochastic rounding errors may be beneficial since choosing a proper rounding strategy eliminates the vanishing gradient problem and forces the rounding bias in a descent direction. Furthermore, we obtain a bound on the convergence rate that is stricter than the one achieved by unbiased stochastic rounding. The theoretical analysis is validated by comparing the performances of various rounding strategies when optimizing several examples using low-precision fixed-point number formats.

Keywords: Fixed-point arithmetic, rounding error analysis, gradient descent, low-precision, stochastic rounding, Polyak–Łojasiewicz inequality

1. Introduction

To reduce computing time and hardware complexity, low-precision numerical formats are becoming increasingly popular, especially in the area of machine learning. A large group of machine learning problems are solved using gradient descent methods (GD), owing to their computational efficiency and stable convergence. GD has a sublinear convergence for convex problems and it has been shown to have linear convergence for both strongly convex problems (Nesterov, 2003) and problems satisfying the *Polyak–Łojasiewicz inequality* (PL) (Polyak, 1963; Łojasiewicz, 1963; Karimi et al., 2016). Strongly convex functions also satisfy the PL condition; see (Karimi et al., 2016, Appendix B). The PL condition has been recently analyzed by Karimi et al. (2016) for optimization problems in machine learning, e.g., least squares and logistic regression. Recent works also show that a wide range of neural networks satisfy the PL condition (Charles and Papailiopoulos, 2018; Nguyen and Mondelli, 2020; Frei and Gu, 2021) and variants thereof (Liu et al., 2022).

*. Version January 2023

Previous work. When the rounding to the nearest method (RN) causes stagnation of training neural networks (NNs), the utilization of low precision with unbiased stochastic rounding, that we call *stochastic rounding* (SR), has been experimentally shown to provide similar training accuracy to single-precision computation; see, e.g., Gupta et al. (2015); Na et al. (2017); Ortiz et al. (2018); Wang et al. (2018). In our previous work (Xia et al., 2022), we have analyzed the influence of stochastic *floating-point* roundoff error on the convergence of GD in low-precision computation for *convex* problems. We have provided a theoretical justification for the reason that SR can help prevent the stagnation of GD in low-precision computation. Moreover, we have proven that the employment of SR results in a similar convergence rate to that of GD with exact arithmetic. We have introduced two new stochastic rounding methods, namely ε -*biased stochastic rounding* (SR_ε) and *signed-SR* $_\varepsilon$, for the various rounding steps in floating-point operations, which are demonstrated, both theoretically and practically, to achieve faster convergence than SR. As an example, Fig. 1 shows the mean value of testing errors of training a multinomial logistic regression model (MLR) using different rounding methods. The application of signed-SR $_\varepsilon$ with a 8-bit number format (Binary8) (Xia et al., 2022, Sec. 2.1) dramatically accelerates the convergence of GD compared to that obtained with SR with Binary8 and RN with single-precision computation (Binary32).

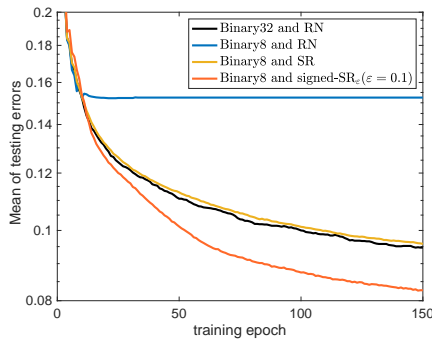


Figure 1: Mean of testing errors of training a MLR on MNIST dataset over 20 simulations using Binary32 with RN and Binary8 with RN, SR, and signed-SR $_\varepsilon$.

Contributions of the paper. In this paper, we study the influence of the *fixed-point* rounding errors on the convergence of GD for problems satisfying the PL condition. Here the stagnation of the algorithm is caused by the absolute rounding errors, hence the analysis is significantly different from the one concerning the stagnation in the floating-point case. We demonstrate that the customized sign of the rounding bias, which has been the main motivation for introducing signed-SR $_\varepsilon$ in Xia et al. (2022), is not necessary in the case of fixed-point arithmetic. In particular, SR $_\varepsilon$ and signed-SR $_\varepsilon$ result in the same rounding bias when choosing the same ε . We prove that, for both SR and SR $_\varepsilon$, the linear convergence rate of GD under the PL condition is preserved for low-precision fixed-point computations and that GD with SR $_\varepsilon$ satisfies a stricter convergence bound than that of GD with SR. We compare the influence of fixed-point and floating-point rounding errors on the convergence of GD. The comparison illustrates that SR $_\varepsilon$ with low-precision floating-point

computation performs as a gradient descent method with automatically adapted stepsizes in each coordinate of the current iterate, while SR_ε with low-precision fixed-point computation behaves as a combination of vanilla gradient descent and a stochastic sign gradient descent method.

Notations. We denote the Euclidean norm and infinity norm by $\|\cdot\|$ and $\|\cdot\|_\infty$, respectively. We indicate by $\mathbb{F} \subseteq \mathbb{R}$ the subset of the real numbers that are exactly representable within the chosen number representation system. Specifically, given a real number $x \in \mathbb{R}$ and a rounding method, $\tilde{x} \in \mathbb{F}$ is used to denote a corresponding fixed-point representation (which is not unique in case of stochastic rounding). We denote by L the Lipschitz constant and by χ the largest distance between the iterates generated by GD and the minimizer, i.e., $\chi := \max_{j=1,\dots,k} \|\mathbf{x}^{(j)} - \mathbf{x}^*\|$ where $\mathbf{x}^{(j)} \in \mathbb{R}^n$. Furthermore, the rounding precision is indicated by u . We employ \simeq and \lesssim to denote approximate equality and inequality with error bounded up to second and higher-order terms in u and a hidden constant with at most polynomial dependence on n , L , and χ .

1.1 Problem settings

Let us briefly recall the convergence behavior of GD for the problems with Lipschitz continuous gradients and satisfying the PL inequality. We consider an unconstrained optimization problem for a differentiable function f with a non-empty solution set \mathcal{X}^* , given by

$$\arg \min_{\mathbf{x} \in \mathbb{R}^n} f(\mathbf{x}),$$

where f satisfies the following assumption.

Problem Assumption. Let $f : \mathbb{R}^n \rightarrow \mathbb{R}$ be a differentiable function whose gradient $\nabla f : \mathbb{R}^n \rightarrow \mathbb{R}^n$ is Lipschitz continuous with constant $L > 0$ and f satisfies the PL inequality with constant $0 < \mu \leq \frac{1}{2}L$.

Denote the corresponding optimal function value of \mathcal{X}^* by f^* . Problem Assumption indicates that f satisfies

$$\|\nabla f(\mathbf{x}) - \nabla f(\mathbf{y})\| \leq L \|\mathbf{x} - \mathbf{y}\|, \tag{1}$$

$$2\mu (f(\mathbf{x}) - f^*) \leq \|\nabla f(\mathbf{x})\|^2. \tag{2}$$

For quadratic functions $f(\mathbf{x}) = \frac{1}{2} \mathbf{x}^T A \mathbf{x}$, where A is symmetric positive definite, μ and L can be taken as the smallest and largest eigenvalue of A , respectively. In particular, the equality $\mu = L$ is attained when A is taken as the identity matrix. For general twice continuously differentiable functions it holds that $\mu \leq L$, which we can see as follows. For this argument, we may assume without loss of generality that $f^* = 0$ and $\mathbf{0} \in \mathcal{X}^*$. Using the Taylor series in this point, we get

$$\mu \mathbf{x}^T \nabla^2 f(\mathbf{0}) \mathbf{x} + \mathcal{O}(\|\mathbf{x}\|^3) = 2\mu f(\mathbf{x}) \leq \|\nabla f(\mathbf{x})\|^2 \leq L^2 \|\mathbf{x}\|^2.$$

If L is sharp, by taking \mathbf{x} in the direction of the largest eigenvalue of $\nabla^2 f(\mathbf{0})$ in modulus, we conclude $\mu \leq L$. Usually, μ will be considerably smaller than L . For the readability of our results, it turns out convenient to assume that $\mu \leq \frac{1}{2}L$; we have therefore added this condition to Problem Assumption. We point out that this is not a restriction; slightly

modified results hold without this extra clause. For instance, for some results instead of $t \leq \frac{1}{L}$, we need $t \leq \min\{\frac{1}{L}, \frac{1}{2\mu}\}$. As explained in (Karimi et al., 2016), (2) implies that every stationary point $\mathbf{x}^* \in \mathcal{X}^*$ is a global minimum. Therefore, a unique globally optimal solution is not implied by our assumption. We remark that, our statements hold with weaker assumptions, for instance by requiring that Problem Assumption is only valid in a certain domain that contains all the iterates of GD.

In exact arithmetic, GD updates iteratively in the opposite direction of the gradient, given by

$$\mathbf{x}^{(k+1)} = \mathbf{x}^{(k)} - t \nabla f(\mathbf{x}^{(k)}), \quad (3)$$

where $t \in \mathbb{R}$ is the *stepsize*. When optimizing problems satisfying Problem Assumption using GD in exact arithmetic, a linear convergence rate is proven by Polyak (1963). A simple version of this proof is given by Karimi et al. (2016).

Theorem 1 (Karimi et al., 2016, Thm. 1) *Let the objective function f satisfy Problem Assumption. In exact arithmetic, the k th iteration step of the gradient descent method with a fixed stepsize $t \leq \frac{1}{L}$ satisfies the following inequality:*

$$f(\tilde{\mathbf{x}}^{(k)}) - f^* \leq (1 - t\mu)^k (f(\mathbf{x}^{(0)}) - f^*). \quad (4)$$

Throughout the paper, we assume that there is no overflow and, to facilitate the convergence analysis, we assume that both the stepsize t and the starting point $\mathbf{x}^{(0)}$ are fixed-point numbers. Under these assumptions, there are only two major types of rounding errors in GD's iteration, i.e., we can write the updating rule of GD with fixed-point arithmetic as

$$\tilde{\mathbf{x}}^{(k+1)} = \tilde{\mathbf{x}}^{(k)} - t \nabla f(\tilde{\mathbf{x}}^{(k)}) - t \boldsymbol{\sigma}_1^{(k)} - \boldsymbol{\sigma}_2^{(k)}, \quad (5)$$

where $\boldsymbol{\sigma}_1^{(k)}$ and $\boldsymbol{\sigma}_2^{(k)}$ are the absolute rounding errors caused by evaluating $\nabla f(\tilde{\mathbf{x}}^{(k)})$ and multiplying the evaluated gradient by t in a limited precision, respectively.

We analyze the influence of rounding errors on the convergence of GD concerning two aspects of the method: monotonicity and convergence rate with respect to the objective function value. Depending on the relation between the magnitudes of the gradients and the rounding precision, we identify three cases, i.e., the case when the updating vectors of GD are fully comprised of scaled gradients components (Case I), the case when the updating vectors of GD are fully dependent on the rounding errors (Case II), and the case when the updating vectors of GD are both dependent on the scaled gradients components and the rounding errors (Case III). Among the three cases, Case I is the one which most likely describes the updating procedure of GD in the initial iteration steps, when the starting point is far from the optimal point. Cases II and III apply to situations where the gradient has some or all components close to the rounding precision u . For all the three cases, we assume that each coordinate of the gradient function is assessed with a **non-opposite sign** (cf. Definition 2) to their exact values. Therefore, the convergence of GD is proven to be guaranteed at least until each coordinate of the gradient function is close to the level of u , i.e., $\|\nabla f\| = \mathcal{O}(\sqrt{nu})$. We prove that in Case I, the employment of SR with low-precision computation leads to the same linear convergence bound, in expectation, as the exact computation for the problems satisfying the PL condition. For Cases II and III, the convergence bound of GD may be slightly larger than the one for exact computations.

When SR_ε is employed, we prove that a stricter convergence bound is obtained than that concerning SR and may be even stricter than the one that applies to exact computation.

1.2 Main theoretical contributions

To gain a better insight on the main contributions of our paper, let us explore the bound of convergence rate by an example. We assume that the objective function f , under Problem Assumption, is optimized using GD with fixed-point arithmetic; from the start to the k_1 th iteration the updating rule satisfies Case I, from $(k_1 + 1)$ st to k_2 th iteration it satisfies Case II, and from $(k_2 + 1)$ st to k_3 th iteration it satisfies Case III. Note that, the assumed order of each case aims at simplifying the example; cases may have different orders and the theoretical result is applicable to any order. If both σ_1 and σ_2 in (5) are computed using SR with fixed stepsize $t < \frac{1}{4L}$, then in view of Corollary 12, Proposition 14, and Proposition 17, the convergence rate satisfies

$$\mathbb{E} [f(\tilde{\mathbf{x}}^{(k)}) - f^*] \lesssim (1 - \mu t)^{k_1} \prod_{j=k_1+1}^{k_2} (1 - \mu t \theta_j) \prod_{j=k_2+1}^{k_3} (1 - \mu(t + \alpha_j)) \cdot (f(\mathbf{x}^{(0)}) - f^*).$$

where all the factors, apart from $f(\mathbf{x}^{(0)}) - f^*$, belong to $[0, 1]$. If σ_1 is computed by SR and σ_2 is computed using SR_ε in (5) with fixed stepsize $t < \frac{1}{4L}$, then based on Theorem 11, Proposition 16, and Proposition 18, the convergence rate satisfies

$$\begin{aligned} & \mathbb{E} [f(\tilde{\mathbf{x}}^{(k)}) - f^*] \\ & \lesssim (1 - \mu(t + \tau_1))^{k_1} \prod_{j=k_1+1}^{k_2} (1 - \mu \theta_j (t + \tau_2)) \prod_{j=k_2+1}^{k_3} (1 - \mu(t + \alpha_j + \theta_j \tau_2)) \cdot (f(\mathbf{x}^{(0)}) - f^*), \end{aligned}$$

where $0 < \varepsilon < 1$ is the parameter in SR_ε introduced in (8) and $0 < \tau_1, \tau_2 \leq 2t\varepsilon$. In particular, the presence of τ_1, τ_2 suggests the faster convergence of the method when SR_ε replaces SR for rounding the multiplication between the gradient and the stepsize. Detailed discussions on τ_1 and τ_2 are given in Proposition 16, and Proposition 18, respectively.

A summary of all the theoretical results with respect to different cases is given in Table 1. Note that, we only consider the use of SR when evaluating gradients. The reason is that SR ensures an estimation of the gradient with a non-opposite sign compared to the exact arithmetic and this property is crucial for the theoretical analysis. In contrast, ensuring the latter property with SR_ε appears difficult in our setting.

1.3 Outline of the paper

Section 2 reviews the basic properties of fixed-point arithmetic and the rounding rules that will be used in this paper. There, we identify the non-opposite sign property to guarantee the descent direction of rounding errors when implementing GD in low-precision computation. In Section 3, the rounding errors are analyzed with respect to its sign and magnitude. Based on the magnitude of rounding errors, we categorize the updating vector of GD into the three cases that we already mentioned in Subsection 1.1. In Section 4, the influence of the rounding bias on the convergence of GD is studied for the problems satisfying Problem Assumption for each of the three cases. Section 5 compares the influence of rounding bias

Table 1: Summary of the theoretical results.

Case	Result	Rounding strategy	Reference
I	Convergence rate	General	Theorem 9
	Convergence rate	$\sigma_1(\text{SR})$ and $\sigma_2(\text{SR}_\varepsilon)$	Theorem 11
	Convergence rate	$\sigma_1(\text{SR})$ and $\sigma_2(\text{SR})$	Corollary 12
II	Monotonicity	$\sigma_1(\text{SR})$ and $\sigma_2(\text{SR})$	Proposition 13
	Convergence rate	$\sigma_1(\text{SR})$ and $\sigma_2(\text{SR})$	Proposition 14
	Monotonicity	$\sigma_1(\text{SR})$ and $\sigma_2(\text{SR}_\varepsilon)$	Proposition 15
	Convergence rate	$\sigma_1(\text{SR})$ and $\sigma_2(\text{SR}_\varepsilon)$	Proposition 16
III	Convergence rate	$\sigma_1(\text{SR})$ and $\sigma_2(\text{SR})$	Proposition 17
	Convergence rate	$\sigma_1(\text{SR})$ and $\sigma_2(\text{SR}_\varepsilon)$	Proposition 18

on the convergence of GD in floating-point and fixed-point arithmetic. We validate our theoretical findings with several numerical simulations in Section 6. Finally, conclusions are drawn in Section 7.

2. Number representation and rounding schemes

Let us introduce fixed-point arithmetic and review the definitions of different rounding methods: RN, SR, SR_ε and signed- SR_ε . Then, we define the non-opposite sign property for the rounded values that will be used to guarantee the descent direction in GD.

2.1 Fixed-point representation

Fixed-point arithmetic is an alternative way to represent numbers in the low-cost embedded microprocessors and microcontrollers, where a floating-point unit is unavailable. Fixed-point numbers are mostly in base 2 (binary representation). We utilize the format $Q[\text{QI}].[\text{QF}]$ to represent binary fixed-point numbers and use the two's complement for the sign, where QI denotes the number of integer bits and QF denotes the number of fractional bits (Oberstar, 2007). For instance, a Q4.6 number presents a 10-bit value with 4 integer bits and 6 fractional bits. Note that, $u = 2^{-\text{QF}}$. The fixed-point arithmetic used in the numerical experiment, is implemented using Matlab's `fi` toolbox.

2.2 Review of rounding methods

When converting a real number to a fixed-point number format, we denote by $\text{fi}(\cdot)$ a general rounding operator that maps $x \in \mathbb{R}$ to $\text{fi}(x) \in \mathbb{F}$. Throughout this study, we consider rounding schemes of the form

$$\text{fi}(x) = \begin{cases} \lfloor x \rfloor, & \text{with probability } p(x), \\ \lfloor x \rfloor + u, & \text{with probability } 1 - p(x), \end{cases} \quad (6)$$

with $p(x) \in [0, 1]$, and $\lfloor x \rfloor = \max\{y \in \mathbb{F} : y \leq x\}$ indicating the largest representable fixed-point number less than or equal to x . When a specific rounding scheme is applied, $\text{fi}(\cdot)$ is replaced by the corresponding rounding operator.

Rounding to the nearest method with half to even (RN) is the default rounding mode used in IEEE 754 floating-point operations. It forces the least significant bit (LSB) to 0 in the case of a tie (Santoro et al., 1989). When we use RN as the rounding operator ($\text{fi} = \text{RN}$) in (6), we have $p_r(x) = 1$ when $x - \lfloor x \rfloor < \frac{1}{2}u$ or when $x - \lfloor x \rfloor = \frac{1}{2}u$ and LSB of $\lfloor x \rfloor$ is even.

Unbiased stochastic rounding (SR) provides an unbiased rounded result by setting a probability that is proportional to the distance from x to the nearest representable fixed-point number. Some basic properties and the backward error analysis of SR have recently been studied by Connolly et al. (2021). When SR is employed as the rounding operator ($\text{fi} = \text{SR}$) in (6), we have

$$p_0(x) = 1 - (x - \lfloor x \rfloor)/u. \quad (7)$$

ε -biased stochastic rounding (SR_ε) has been introduced by Xia et al. (2022). It provides a rounding bias with the same sign as its input by increasing or decreasing by $\varepsilon \in (0, 1)$ the probability of rounding down in SR, depending on the sign of the input number (cf. (8b)). When we choose SR_ε as the rounding operator ($\text{fi} = \text{SR}_\varepsilon$) in (6), we have

$$p_\varepsilon(x) := \varphi(\eta(x, \varepsilon)), \quad (8a)$$

with

$$\eta(x, \varepsilon) := 1 - (x - \lfloor x \rfloor)/u - \text{sign}(x) \varepsilon, \quad \varphi(y) = \begin{cases} 0, & y \leq 0, \\ y, & 0 \leq y \leq 1, \\ 1, & y \geq 1. \end{cases} \quad (8b)$$

Signed- SR_ε is a variant of SR_ε where we can customize the sign of the rounding bias by replacing $\text{sign}(x)$ in (8b) with the sign of the additional variable $v \in \mathbb{R}$, i.e.,

$$\tilde{p}_\varepsilon(x) := \varphi(\tilde{\eta}(x, \varepsilon, v)), \quad (9a)$$

with

$$\tilde{\eta}(x, \varepsilon, v) := 1 - (x - \lfloor x \rfloor)/u - \text{sign}(v) \varepsilon. \quad (9b)$$

A detailed description of SR_ε and signed- SR_ε , and their implementations, can be found in (Xia et al., 2022, Sec. 2.2). We will use all four rounding methods for the convergence analysis in Section 4 and Section 5.

2.3 Preserving non-opposite sign of fixed-point arithmetic operations

Under the assumption that there is no overflow, addition, and subtraction of fixed-point numbers, within the same number format, do not introduce any rounding errors. However, representing the product of two fixed-point numbers may require more digits than those used for representing the factors (Yates, 2009); e.g., multiplying two 8-bit values produces

a 16-bit result, in general. In the case of multiplication, we adopt the following model to present the rounded value

$$\text{fi}(\tilde{x}\tilde{y}) = \tilde{x}\tilde{y} + \sigma, \quad \text{where } \begin{cases} |\sigma| < u & \text{for SR, SR}_\varepsilon \text{ and signed-SR}_\varepsilon, \\ |\sigma| \leq \frac{1}{2}u & \text{for RN,} \end{cases} \quad (10)$$

where $\text{fi} \in \{\text{RN}, \text{SR}, \text{SR}_\varepsilon, \text{signed-SR}_\varepsilon\}$ and $\text{fi}(\tilde{x}\tilde{y}) \in ([\tilde{x}\tilde{y}], [\tilde{x}\tilde{y}] + u)$. The main difference between (10) and the model of floating-point computation (Higham, 2002, Sec. 2.1) is that the rounding error σ is ensured to be small only in an absolute sense. Due to the rounding properties, we always have $\text{sign}(\text{fi}(\tilde{x}\tilde{y})) \text{sign}(\tilde{x}\tilde{y}) \geq 0$. Specifically, for a single operation, all the rounding schemes mentioned in Section 2.2 will not result in a rounded value with an opposite sign as its input.

However, this may be different when a series of operations is carried out. For instance, using SR to compute $\text{fi}(0.24) - \text{fi}(0.26)$ within the binary number format Q1.1 ($u = 2^{-1}$), we have

$$\text{SR}(0.24) - \text{SR}(0.26) = \begin{cases} 0.5, & \text{with probability 0.2304,} \\ 0, & \text{with probability 0.4992,} \\ -0.5, & \text{with probability 0.2704.} \end{cases}$$

Similar issues are encountered in deterministic rounding. Despite RN being monotonic, i.e., $x \leq y \in \mathbb{R}$ implies $\text{RN}(x) \leq \text{RN}(y)$, when more than two rounding errors are accumulated, an opposite sign may be obtained; for instance, within the number format Q1.1, we have

$$\text{sign}(\text{RN}(0.26) + \text{RN}(-0.24) + \text{RN}(-0.24)) = -\text{sign}(0.26 - 0.24 - 0.24).$$

In Section 3.1, we will see that it is crucial to ensure that the rounded gradient preserves the sign of the exact gradient componentwise, as this leads GD to update in a non-ascent direction. For this reason, we introduce the property of *non-opposite sign* for the rounded outcome of a sequence of operations in a specific number format.

Definition 2 (non-opposite sign) *When evaluating $g(x) : \mathbb{R}^n \rightarrow \mathbb{R}$ in fixed-point arithmetic, we say that the resulting value $\widetilde{g(x)}$ has the non-opposite sign property if*

$$\text{sign}(\widetilde{g(x)}) \text{sign}(g(x)) \geq 0.$$

To facilitate further analysis, we propose a condition to guarantee the non-opposite sign property for RN and stochastic rounding methods. Denote by σ_g the accumulated rounding error in evaluating $g(x)$, such that $\widetilde{g(x)} = g(x) + \sigma_g$. If

$$|g(x)| \geq |\sigma_g|, \quad (11)$$

then it easily follows that $\widetilde{g(x)}$ has the non-opposite sign property. Now, we analyze what happens in expectation to the sign of stochastically rounded quantities. In the case of SR, we demonstrate that the zero mean property implies the non-opposite sign in expectation when $g(x) \geq cu^2$.

Proposition 3 *Let $g : \mathbb{R}^n \rightarrow \mathbb{R}$ be a function that can be evaluated with a finite sequence of the elementary operations $(+, -, *, /)$, and let $\widetilde{g(\mathbf{x})}$ be the corresponding random variable obtained by evaluating the operations using fixed-point arithmetic and SR for rounding. Then*

$$|\mathbb{E}[\widetilde{g(\mathbf{x})}] - g(\mathbf{x})| \lesssim c \cdot \mathcal{O}(u^2), \quad (12)$$

where c depends on the point \mathbf{x} and the number of multiplications and divisions performed for evaluating $g(\mathbf{x})$.

Proof Let σ_g denote the accumulated error caused by evaluating g so that $\widetilde{g(\mathbf{x})} = g(\mathbf{x}) + \sigma_g$. If the evaluation of $g(\mathbf{x})$ requires m elementary operations, then considering the Taylor expansion of the accumulated error, in accordance with (Linnainmaa, 1976, (8)), we have

$$\sigma_g = \sum_{i=1}^m c_{m,i} \sigma_i + \sum_{i=1}^m \sum_{j=1}^i c_{m,ij} \sigma_i \sigma_j + \mathcal{O}(u^3),$$

where σ_i, σ_j indicate the error introduced by single operations and $c_{m,i}, c_{m,ij}$ are certain scalar coefficients. The zero mean independence property (Connolly et al., 2021, Lemma 5.2) implies that $\mathbb{E}[\sigma_i] = 0$ and $\mathbb{E}[\sigma_i \sigma_j] = 0$ for $i \neq j$. Therefore, we achieve

$$|\mathbb{E}[\sigma_g]| \leq \sum_{i=1}^n |c_{n,ii}| \sigma_i^2 \leq c u^2,$$

where c is problem dependent and can be obtained based on Table 1 in (Linnainmaa, 1976). Note that Table 1 in (Linnainmaa, 1976) is based on floating-point arithmetic; when fixed-point arithmetic is applied, only the coefficients in multiplication and division operations are relevant. ■

Remark 4 *For instance, when $g(\mathbf{x}) = x_1^2 + x_1 x_2$, based on the Taylor expansion and Table 1 in (Linnainmaa, 1976), the accumulated error can be expressed as $\sigma_g = 2x_1 \sigma_{x_1} + x_2 \sigma_{x_1} + x_1 \sigma_{x_2} + \sigma_{x_1}^2 + \mathcal{O}(u^3)$, where the constant in front of $\sigma_{x_1}^2$ is obtained from the 5th row and column in Table 1 in (Linnainmaa, 1976). Therefore, using SR, the expectation of the accumulated error is bounded by $\mathbb{E}[\sigma_g] \leq u^2$.*

Therefore, when using SR and $g(\mathbf{x}) \geq c u^2$, we have that $\mathbb{E}[\widetilde{g(\mathbf{x})}]$ has a non-opposite sign with respect to $g(\mathbf{x})$. However, this property cannot be guaranteed by SR_ε . In the next section, we analyze the influence of rounding errors on the convergence of GD under the PL condition for different rounding strategies on the basis of (11) and Proposition 3.

3. Gradient descent method with fixed-point arithmetic

Depending on different optimization problems, near the optimum, the algorithm may move back and forth around the minimum repeatedly; see e.g., (Boyd and Vandenberghe, 2004, Figure 9.2). This zigzag behavior is generally caused by the rapid change in negative

gradient direction and can be mitigated by reducing the stepsize (setting a smaller t) or adding a momentum term; see, e.g., the heavy ball method Polyak (1964) and Nesterov's accelerated method (Nesterov, 2003, (2.2.11)). Although reducing the stepsize mitigates the zigzag behavior, when implementing GD in low precision and RN, a small stepsize may prevent GD to converge because of the loss of gradient information. This issue is known as vanishing gradient problem and can be overcome by means of stochastic rounding strategies (Gupta et al., 2015; Xia et al., 2022). We start our convergence analysis by studying the role of rounding errors during the updating procedure of GD for fixed-point arithmetic.

A key tool for our analysis is the *updating vector* of GD (cf. (5))

$$\mathbf{d}^{(k)} := t \nabla f(\tilde{\mathbf{x}}^{(k)}) + t \boldsymbol{\sigma}_1^{(k)} + \boldsymbol{\sigma}_2^{(k)}.$$

Therefore, we obtain the following general expression for GD's iteration:

$$\tilde{\mathbf{x}}^{(k+1)} = \tilde{\mathbf{x}}^{(k)} - \mathbf{d}^{(k)}. \quad (13)$$

From (10), we have that $\|\boldsymbol{\sigma}_1^{(k)}\|_\infty \leq mu$, where m is a positive constant depending on the gradient function and $\tilde{\mathbf{x}}$; $\|\boldsymbol{\sigma}_2^{(k)}\|_\infty \leq \frac{1}{2}u$ and $\|\boldsymbol{\sigma}_2^{(k)}\|_\infty < u$ for RN and stochastic rounding, respectively. In particular, both signs of the elements and magnitude of $\mathbf{d}^{(k)}$ are crucial to understand the convergence of GD. In the next subsection, we distinguish three cases that describe the number of components of the updating vector that have magnitudes close to the rounding errors. We explore the roles of $\boldsymbol{\sigma}_1^{(k)}$ and $\boldsymbol{\sigma}_2^{(k)}$ in determining properties of $\mathbf{d}^{(k)}$. We start by studying a condition that ensures that $\mathbf{d}^{(k)}$ has an ascent direction.

3.1 A condition for the non-opposite sign property

Intuitively, it is desirable to have that the entries of $\mathbf{d}^{(k)}$ have non-opposite signs to the corresponding entries of $\nabla f(\tilde{\mathbf{x}}^{(k)})$, as this property implies that $\mathbf{d}^{(k)}$ has a non-ascent direction. Taking a closer look at (5) we see that $\boldsymbol{\sigma}_2^{(k)}$, which originates from a multiplication, can not result in an opposite sign. On the other hand, in view of (10), $\boldsymbol{\sigma}_1^{(k)}$ plays a significant role whenever one or some of the entries of the exact gradient verify $|\nabla f(\tilde{\mathbf{x}}^{(k)})_i| < |\sigma_{1,i}^{(k)}|$. In this case, GD may still update in a descent direction when $\nabla f(\tilde{\mathbf{x}}^{(k)})^T \mathbf{d}^{(k)} > 0$; however, we cannot guarantee the monotonicity of the objective function values in general and, often, zigzag behavior is observed in the neighborhood of the optimal points.

Therefore, our analysis is restricted to those iterations that satisfy:

$$|\nabla f(\tilde{\mathbf{x}}^{(k)})_i| \geq |\sigma_{1,i}^{(k)}|, \quad i = 1, \dots, n. \quad (14)$$

In this situation, GD is ensured to update in a descent direction as (14) implies that

$$\text{sign}(t \nabla f(\tilde{\mathbf{x}}^{(k)})_i) \text{sign}(t \nabla f(\tilde{\mathbf{x}}^{(k)})_i + t \sigma_{1,i}^{(k)} + \sigma_{2,i}^{(k)}) \geq 0 \quad i = 1, \dots, n.$$

Note that, condition (14) is a very reasonable assumption, as it indicates that the rounding error in evaluating the gradient should not be larger than the true quantity. Together with the Lipschitz continuity property in Problem Assumption, (14) implies the lower bound $\|\tilde{\mathbf{x}}^{(k)} - \mathbf{x}^*\| \geq L^{-1} \|\boldsymbol{\sigma}_1^{(k)}\|$, which means that the method may not get arbitrarily close to the optimal point. In Section 6.3, we show an example where GD converges to the exact optimal point when it is representable in a finite precision, and otherwise converges to a neighborhood of the optimal point whose size depends on u .

3.2 Recap of the general assumptions

So far, we have discussed several reasonable assumptions concerning the objective function, the number format, and the rounding operation. To get concise statements in our convergence analysis and to make it easier for the reader to retrieve these properties, in the following we recap the conditions assumed for all the theoretical statements in this paper.

Universal Assumptions.

1. The objective function f satisfies Problem Assumption.
2. The evaluation of the components of ∇f satisfies the assumption of Proposition 3. Moreover, the parameter c depends only and at most polynomially on n, L, χ .
3. For every iteration step, the absolute error $\sigma_1^{(k)}$ caused by evaluating the gradient satisfies (14).
4. The quantities $\mathbf{x}^{(0)}$ and t are exactly represented in finite-precision.
5. All the iterates generated by GD are in a compact space such that $\|\mathbf{x}^{(k)} - \mathbf{x}^*\| \leq \chi$.
6. Overflow is never encountered during computations.

Note that the Universal Assumptions 1. and 5. imply that $\|\nabla f(\mathbf{x}^{(k)})\| \leq L\chi$.

3.3 The magnitude of the updating vector

Together with the non-opposite sign property of the previous subsection, the magnitude of the entries of $\mathbf{d}^{(k)}$ is crucial for studying the convergence properties of GD. However, during the execution of GD it is reasonable to observe different magnitudes among the various components of the gradient. For this reason, we identify and subdivide our theoretical analysis for the following three cases.

Condition of Case I.

$$|\nabla f(\tilde{\mathbf{x}}^{(k)})_i + \sigma_{1,i}^{(k)}| \geq \frac{u}{t}, \quad i = 1, \dots, n. \quad (15)$$

Condition of Case II.

$$|\nabla f(\tilde{\mathbf{x}}^{(k)})_i + \sigma_{1,i}^{(k)}| < \frac{u}{t}, \quad i = 1, \dots, n. \quad (16)$$

Condition of Case III. There exist disjoint non-empty subsets of indices $\mathcal{C}_1, \mathcal{C}_2$ such that $\mathcal{C}_1 \cup \mathcal{C}_2 = \{1, \dots, n\}$ and

$$|\nabla f(\tilde{\mathbf{x}}^{(k)})_i + \sigma_{1,i}^{(k)}| \geq \frac{u}{t}, \quad \text{for } i \in \mathcal{C}_1, \quad |\nabla f(\tilde{\mathbf{x}}^{(k)})_i + \sigma_{1,i}^{(k)}| < \frac{u}{t}, \quad \text{for } i \in \mathcal{C}_2. \quad (17)$$

Considering the general expression for GD's iteration (13), we can reformulate $\mathbf{d}^{(k)}$ with respect to these three conditions.

Case I. In this case the magnitude of the i th component of $\mathbf{d}^{(k)}$ (cf. (15)) mainly depends on $\nabla f(\tilde{\mathbf{x}}^{(k)})_i$ and we informally say that *the updating procedure of GD is dominated by the gradient*. Let us rewrite the updating vector as

$$\mathbf{d}^{(k)} = t \nabla f(\tilde{\mathbf{x}}^{(k)}) \circ (\mathbf{1} + \mathbf{r}^{(k)}), \quad (18)$$

where \circ is the Hadamard (component-wise) product and $\mathbf{r}^{(k)}$ is a vector of the relative errors with respect to the exact quantity $t \nabla f(\tilde{\mathbf{x}}^{(k)})$, whose entries are given by

$$r_i^{(k)} = \frac{t \sigma_{1,i}^{(k)} + \sigma_{2,i}^{(k)}}{t \nabla f(\tilde{\mathbf{x}}^{(k)})_i}, \quad \text{for } i = 1, \dots, n. \quad (19)$$

Equations (14) and (15) imply bounds on the entries of $\mathbf{r}^{(k)}$; indeed, we have the following result.

Lemma 5 *Under the Universal Assumptions and the condition of Case I (cf. (15)), we have that*

$$-1 \leq r_i^{(k)} \leq 3, \quad \text{for } i = 1, \dots, n.$$

The proof is available in Appendix A.

Case II. Condition (16) shows that $\sigma_2^{(k)}$ has a crucial impact on determining the magnitude of $\mathbf{d}^{(k)}$. All the entries of the updating vector belong to the set $\{0, u, -u\}$ and, if RN is employed, it is likely that GD stagnates. In this case, *the updating procedure of GD is dominated by the rounding errors*. The updating vector is generated according to the rule

$$d_i^{(k)} = \begin{cases} 0, & \text{with probability } p(t \nabla f(\mathbf{x}^{(k)})_i + t \sigma_{1,i}^{(k)}), \\ \text{sign}(\nabla f(\mathbf{x}^{(k)})_i + \sigma_{1,i}^{(k)}) u, & \text{with probability } 1 - p(t \nabla f(\mathbf{x}^{(k)})_i + t \sigma_{1,i}^{(k)}), \end{cases} \quad (20)$$

where $p \in \{p_r, p_0, p_\varepsilon, \tilde{p}_\varepsilon\}$ depending on which of the rounding methods introduced in Section 2.2 is employed. This updating rule is similar to what happens in the *sign gradient descent method* by Moulay et al. (2019), except for the stochastic dependence of our scheme.

Case III. This last case refers to the situation where the components of the gradient vector have different scales so that we have some entries on the level of the rounding error and others close to the value of the exact partial derivative. We informally say that *the updating procedure of GD is partially dominated by the gradient and partially dominated by the rounding errors*. More explicitly, in Case III the updating vector is generated as follows:

$$i \in \mathcal{C}_1 \Rightarrow d_i^{(k)} = t \nabla f(\tilde{\mathbf{x}}^{(k)})_i (1 + r_i^{(k)}); \quad (21)$$

$$i \in \mathcal{C}_2 \Rightarrow d_i^{(k)} = \begin{cases} 0, & \text{with probability } p(t \nabla f(\mathbf{x}^{(k)})_i + t \sigma_{1,i}^{(k)}), \\ \text{sign}(\nabla f(\mathbf{x}^{(k)})_i + \sigma_{1,i}^{(k)}) u, & \text{with probability } 1 - p(t \nabla f(\mathbf{x}^{(k)})_i + t \sigma_{1,i}^{(k)}), \end{cases}$$

which may be viewed as a combination of (18) and (20). In the next section, we provide an analysis of the convergence of GD for all three cases, regarding two aspects: the monotonicity and the convergence rate.

4. Convergence analysis of GD with fixed-point arithmetic

Under Universal Assumptions, when using stochastic rounding methods, the quantities $\mathbf{d}^{(k)}$, $\mathbf{x}^{(k)}$, and $\nabla f(\tilde{\mathbf{x}}^{(k)})$ can be viewed as random vectors obtained by GD. We prove that for the objective functions satisfying Problem Assumption the linear convergence of GD in exact arithmetic (cf. Theorem 1) can be extended to our framework (cf. (5)). We begin by analyzing the updating direction of rounding errors for different stochastic rounding methods.

4.1 The direction of stochastic rounding errors

Taking the expectation of $\nabla f(\tilde{\mathbf{x}}^{(k)})^T \mathbf{d}^{(k)}$ in (13), we have

$$\begin{aligned} \mathbb{E}[\nabla f(\tilde{\mathbf{x}}^{(k)})^T \mathbf{d}^{(k)}] &= \mathbb{E}[\nabla f(\tilde{\mathbf{x}}^{(k)})^T (t \nabla f(\tilde{\mathbf{x}}^{(k)}) + t \boldsymbol{\sigma}_1^{(k)} + \boldsymbol{\sigma}_2^{(k)})] \\ &= t \mathbb{E}[\|\nabla f(\tilde{\mathbf{x}}^{(k)})\|^2] + t \mathbb{E}[\nabla f(\tilde{\mathbf{x}}^{(k)})^T \boldsymbol{\sigma}_1^{(k)}] + \mathbb{E}[\nabla f(\tilde{\mathbf{x}}^{(k)})^T \boldsymbol{\sigma}_2^{(k)}]. \end{aligned} \quad (22)$$

From (22), we see that both $\boldsymbol{\sigma}_1^{(k)}$ and $\boldsymbol{\sigma}_2^{(k)}$ may result in a different updating direction and distance from the exact updating procedure. One may choose the stepsize t to influence the term $\mathbb{E}[\nabla f(\tilde{\mathbf{x}}^{(k)})^T \boldsymbol{\sigma}_1^{(k)}]$, but the quantity $\mathbb{E}[\nabla f(\tilde{\mathbf{x}}^{(k)})^T \boldsymbol{\sigma}_2^{(k)}]$ is not affected by the choice of t .

Now, we study the quantity $\mathbb{E}[\nabla f(\tilde{\mathbf{x}}^{(k)})^T \boldsymbol{\sigma}_1^{(k)}]$ for different stochastic rounding methods.

Lemma 6 *Under Universal Assumptions, if SR is applied for evaluating $\boldsymbol{\sigma}_1$, then it holds*

$$\mathbb{E}[\nabla f(\tilde{\mathbf{x}}^{(k)})^T (\nabla f(\tilde{\mathbf{x}}^{(k)}) + \boldsymbol{\sigma}_1^{(k)})] \simeq \mathbb{E}[\|\nabla f(\tilde{\mathbf{x}}^{(k)})\|^2],$$

where \simeq is defined in Section 1.

The proof is available in Appendix A and indicates that when $L\chi\sqrt{n}\mathcal{O}(u^2)$ is negligible, SR causes the expectation of the inner product $\nabla f(\tilde{\mathbf{x}}^{(k)})^T \text{SR}(\nabla f(\tilde{\mathbf{x}}^{(k)}))$, to coincide to the corresponding quantity in exact arithmetic, i.e.,

$$\mathbb{E}[\nabla f(\tilde{\mathbf{x}}^{(k)})^T \text{SR}(\nabla f(\tilde{\mathbf{x}}^{(k)}))] \simeq \mathbb{E}[\|\nabla f(\tilde{\mathbf{x}}^{(k)})\|^2].$$

Unfortunately, this is not the case for SR_ε because $\mathbb{E}[\boldsymbol{\sigma}_1]$ is hard to be determined when $\mathbb{E}[\nabla f(\tilde{\mathbf{x}}^{(k)})]$ is unknown. To circumvent this problem-dependent behavior of SR_ε , we only consider the use of SR to evaluate all the gradients in our analysis.

Now, let us study the quantity $\mathbb{E}[\nabla f(\tilde{\mathbf{x}}^{(k)})^T \boldsymbol{\sigma}_2^{(k)}]$; when using SR we have the zero bias property.

Lemma 7 *If SR is applied for evaluating $\boldsymbol{\sigma}_2$, then it holds*

$$\mathbb{E}[\nabla f(\tilde{\mathbf{x}}^{(k)})^T \boldsymbol{\sigma}_2^{(k)}] = 0.$$

We omit the proof of Lemma 7, since it can be simply derived from $\mathbb{E}[\sigma_{2,i}^{(k)} | \nabla f(\tilde{\mathbf{x}}^{(k)})_i, \sigma_{1,i}^{(k)}] = 0$ for all i and utilizing the law of total expectation (e.g., (Biagini and Campanino, 2016, (1.14))).

On the other hand, if we apply SR_ε we obtain, on average, an additional contribution in an ascent direction.

Lemma 8 *If SR_ε is applied for evaluating σ_2 and (14) is satisfied, then it holds*

$$\mathbb{E} [\nabla f(\tilde{\mathbf{x}}^{(k)})^T \sigma_2^{(k)}] > 0.$$

The proof is available in Appendix A. In the next section, we will use the results stated here as building blocks for studying the influence of rounding errors on the convergence of GD.

4.2 Convergence analysis of GD for the three cases

Let us proceed to analyze the convergence of GD in the three cases introduced in Section 3.3. For each case, we provide conditions to ensure that the sequence generated by GD has non increasing objective function values. Moreover, we quantify the rate of convergence on the basis of the number of steps that GD spends in each case.

4.2.1 CASE I

We start by observing that the condition of Case I implies $2t|\nabla f(\tilde{\mathbf{x}}^{(k)})_i| \geq u$, $i = 1, \dots, n$, which leads to

$$\|\nabla f(\tilde{\mathbf{x}}^{(k)})\| \geq \frac{1}{2}\sqrt{n} \frac{u}{t}. \quad (23)$$

In view of (1), (23) implies $\|\mathbf{x}^{(k)} - \mathbf{x}^*\| \geq \frac{1}{2}L^{-1}\sqrt{n} \frac{u}{t}$, where $\mathbf{x}^* \in \mathcal{X}^*$. Together with the inequality (23), it tells us that GD can satisfy the condition of Case I only outside a neighborhood of \mathcal{X}^* .

Next, we will show that with low-precision computations, GD converges to a neighborhood around or even exactly to \mathbf{x}^* with respect to general rounding errors. Denote the minimum ratio between the exact entries and rounded entries of $t\nabla f(\tilde{\mathbf{x}}^{(j)})$ at the j th iterate by

$$\gamma_j := \min_{i=1, \dots, n} 1 + r_i^{(j)},$$

so that $\gamma_j \in [0, 4]$ (see Lemma 5). We commence the study of the objective function values associated with the sequence generated by GD in finite precision. Adapting the proof of (Karimi et al., 2016, Theorem 1) to our framework, we obtain the following result for general rounding errors.

Theorem 9 *Under Universal Assumptions, after k iteration steps of GD in fixed-precision arithmetic with a fixed stepsize t such that $t < \frac{1}{4L}$ and suppose that the condition of Case I has been satisfied throughout the k iteration steps. Then, the k th iterate satisfies:*

$$f(\tilde{\mathbf{x}}^{(k)}) - f^* \leq \prod_{j=0}^{k-1} (1 - t\mu\gamma_j) \cdot (f(\mathbf{x}^{(0)}) - f^*), \quad (24)$$

where $0 < t\mu\gamma_j < \frac{1}{2}$, $j = 0, \dots, k-1$.

Proof The Lipschitz gradient property and (18) allow us to write

$$\begin{aligned} f(\tilde{\mathbf{x}}^{(k+1)}) &\leq f(\tilde{\mathbf{x}}^{(k)}) - \nabla f(\tilde{\mathbf{x}}^{(k)})^T \mathbf{d}^{(k)} + \frac{1}{2}L \|\mathbf{d}^{(k)}\|^2 \\ &= f(\tilde{\mathbf{x}}^{(k)}) - t \sum_{i=1}^n (1 + r_i^{(k)}) \left(1 - \frac{1}{2}Lt(1 + r_i^{(k)})\right) (\nabla f(\tilde{\mathbf{x}}^{(k)})_i)^2. \end{aligned}$$

Since $t < \frac{1}{4L}$ and $0 \leq 1 + r_i^{(k)} \leq 4$ (Lemma 5), we have that

$$f(\tilde{\mathbf{x}}^{(k+1)}) \leq f(\tilde{\mathbf{x}}^{(k)}) - \frac{1}{2} t \sum_{i=1}^n (1 + r_i^{(k)}) (\nabla f(\tilde{\mathbf{x}}^{(k)})_i)^2, \quad (25)$$

which in turn implies

$$\begin{aligned} f(\tilde{\mathbf{x}}^{(k+1)}) - f^* &\leq f(\tilde{\mathbf{x}}^{(k)}) - f^* - \frac{1}{2} t \gamma_k \|\nabla f(\tilde{\mathbf{x}}^{(k)})\|^2 \\ &\stackrel{(2)}{\leq} f(\tilde{\mathbf{x}}^{(k)}) - f^* - t \mu \gamma_k (f(\tilde{\mathbf{x}}^{(k)}) - f^*) \\ &= (1 - t \mu \gamma_k) (f(\tilde{\mathbf{x}}^{(k)}) - f^*). \end{aligned} \quad (26)$$

The assumptions $\mu < \frac{1}{2}L$, $t < \frac{1}{4L}$, and $\gamma_k \leq 4$, yield $1 - t \mu \gamma_k \in (\frac{1}{2}, 1)$. By expanding the recursive definition of (26), we obtain the required result. \blacksquare

Comparing Theorem 1 and Theorem 9, in the presence of rounding errors, a smaller t is required to ensure the monotonicity of GD. In particular, the bound on t depends on the upper bound on the relative rounding errors of $t \nabla f(\tilde{\mathbf{x}}^{(k)})$, i.e., a larger $r_i^{(k)}$ in (19) leads to a smaller bound on t . Moreover, when exact arithmetic is considered, i.e., $\gamma_j = 1$ in (24) for all j , Theorem 9 yields the same convergence rate that holds for infinite-precision computations: $f(\tilde{\mathbf{x}}^{(k)}) - f^* \leq (1 - t \mu)^k (f(\mathbf{x}^{(0)}) - f^*)$ (cf. (4)).

Interestingly, Theorem 9 also states that a faster convergence rate may be achieved when many of the γ_j s are larger than 1 (again, comparing with (4)). Next, we show that we may achieve this, on average, by employing SR_ε for evaluating σ_2 . Before stating the result, we introduce and comment a quantity that is important for our analysis:

$$\rho_k := \min_{i=1, \dots, n} \frac{n \mathbb{E} [\sigma_{2,i}^{(k)} \nabla f(\tilde{\mathbf{x}}^{(k)})_i]}{\mathbb{E} [\|\nabla f(\tilde{\mathbf{x}}^{(k)})\|^2]}. \quad (27)$$

The value of ρ_k measures the minimum ratio between the expected rounding errors and the expected squared norm of the gradient at the k th iteration. According to Lemma 6 and 7, it is easy to check that when SR is applied for evaluating σ_2 , we have $\rho_j = 0$ for $j = 1, \dots, k$. When SR_ε is applied, we can instead rely on the following upper bound.

Lemma 10 *If SR_ε is employed for evaluating σ_2 for the k th iteration step of GD, then we have that $\rho_k \leq 2t\varepsilon$.*

The proof of Lemma 10 is available in the Appendix A. We are now ready to analyze the convergence rate for SR_ε . To facilitate the analysis, let us denote the minimum value of ρ_j over the iteration steps as

$$\tau_1 := \min_{j=0, \dots, k-1} \rho_j. \quad (28)$$

Based on Lemma 10, we have $\tau_1 \in (0, 2t\varepsilon]$.

Theorem 11 *Under Universal Assumptions, after k iteration steps of GD in fixed-precision arithmetic with a fixed stepsize t such that $t < \frac{1}{4L}$ and suppose that the condition of Case I*

is satisfied throughout the k iteration steps. If σ_1 and σ_2 in (5) are obtained using SR and SR_ε , respectively, then we have

$$\mathbb{E}[f(\tilde{\mathbf{x}}^{(k)}) - f^*] \lesssim (1 - (t + \tau_1)\mu)^k (f(\mathbf{x}^{(0)}) - f^*), \quad (29)$$

where $\tau_1 \in (0, 2t\varepsilon]$ is such that $\mu(t + \tau_1) < 1$, and \lesssim is the notation described in Section 1.

Proof Substituting (19) into (25), and taking the expectation of both sides, we obtain

$$\begin{aligned} \mathbb{E}[f(\tilde{\mathbf{x}}^{(k+1)}) - f^*] &\leq \mathbb{E}[f(\tilde{\mathbf{x}}^{(k)}) - f^*] - \frac{1}{2}t \mathbb{E}[\|\nabla f(\tilde{\mathbf{x}}^{(k)})\|^2] \\ &\quad - \frac{1}{2} \sum_{i=1}^n (t \mathbb{E}[\sigma_{1,i}^{(k)} \nabla f(\tilde{\mathbf{x}}^{(k)})_i] + \mathbb{E}[\sigma_{2,i}^{(k)} \nabla f(\tilde{\mathbf{x}}^{(k)})_i]). \end{aligned} \quad (30)$$

In view of Lemmas 6 and 8, we have $\mathbb{E}[\|\nabla f(\tilde{\mathbf{x}}^{(k)})\|^2] + \mathbb{E}[\sigma_{1,i}^{(k)} \nabla f(\tilde{\mathbf{x}}^{(k)})_i] \simeq \mathbb{E}[\|\nabla f(\tilde{\mathbf{x}}^{(k)})\|^2]$ and $\mathbb{E}[\sigma_{2,i}^{(k)} \nabla f(\tilde{\mathbf{x}}^{(k)})_i] > 0$. Further, (27) and (30) imply that

$$\mathbb{E}[f(\tilde{\mathbf{x}}^{(k+1)}) - f^*] \lesssim \mathbb{E}[f(\tilde{\mathbf{x}}^{(k)}) - f^*] - \frac{1}{2}t \mathbb{E}[\|\nabla f(\tilde{\mathbf{x}}^{(k)})\|^2] - \frac{1}{2}\rho_k \mathbb{E}[\|\nabla f(\tilde{\mathbf{x}}^{(k)})\|^2]. \quad (31)$$

Taking the expectation of (2), we obtain

$$\mathbb{E}[\|\nabla f(\tilde{\mathbf{x}}^{(k)})\|^2] \geq 2\mu \mathbb{E}[f(\tilde{\mathbf{x}}^{(k)}) - f^*]. \quad (32)$$

Hence, substituting (32) into (31), we have

$$\mathbb{E}[f(\tilde{\mathbf{x}}^{(k+1)}) - f^*] \lesssim (1 - (t + \rho_k)\mu) \mathbb{E}[f(\tilde{\mathbf{x}}^{(k)}) - f^*].$$

Expanding the recursion, we obtain

$$\mathbb{E}[f(\tilde{\mathbf{x}}^{(k)}) - f^*] \lesssim \prod_{j=0}^{k-1} (1 - (t + \rho_j)\mu) \mathbb{E}[f(\mathbf{x}^{(0)}) - f^*].$$

According to Lemma 10, we have the claim for a certain $\tau_1 \in (0, 2t\varepsilon)$. Furthermore, the properties $\varepsilon < 1$, $\rho_j \leq 2t\varepsilon$ and $\mu \leq L/2$ yield $(t + \rho_j)\mu \leq \frac{1+2\varepsilon}{8} < \frac{3}{8}$. \blacksquare

Looking at (27), a larger ε in SR_ε might allow a larger bound for τ_1 . Comparing Theorem 1 (cf. (4)) and Theorem 11 (cf. (29)), when choosing the same t , we have that a tighter bound on convergence rate, in expectation, is obtained by using SR_ε . When employing SR for both σ_1 and σ_2 , Lemma 7 implies $\mathbb{E}[\sigma_{2,i}^{(k)} \nabla f(\tilde{\mathbf{x}}^{(k)})_i] = 0$, which yields $\rho_k = 0$ in (30). Together with Lemma 6, this gives, in expectation, the same convergence rate that holds for infinite-precision computations.

Corollary 12 *Under the same assumptions of Theorem 11, if SR is applied for computing σ_2 , it holds:*

$$\mathbb{E}[f(\tilde{\mathbf{x}}^{(k)}) - f^*] \lesssim (1 - t\mu)^k (f(\mathbf{x}^{(0)}) - f^*).$$

We omit the proof of Corollary 12, since it can be easily obtained on the basis of Lemma 7 and by proceeding analogously to the proof of Theorem 11. Both Theorem 11 and Corollary 12 require smaller values of t , compared to the exact computations case, for guaranteeing the convergence of GD, since the analysis of them are based on the worst-case bound of σ_1 . In the simulation studies reported in Section 6, we will show that these restrictions are usually pessimistic and, in practice, t can be chosen as large as the upper bound in Theorem 1, that is $t \leq \frac{1}{L}$.

4.2.2 CASE II

In Case II, each of the entry of the updating vector $\mathbf{d}^{(k)}$ takes one of the values in $\{0, u, -u\}$; when it is 0, property (14) implies that $\nabla f(\tilde{\mathbf{x}}^{(k)})_i = 0$. Therefore, we have $\sigma_{2,i} = 0$, which does not influence the convergence of GD. For our analysis it is convenient to single out the cases where the rounded gradient has some components that are exactly zero. More formally, we denote the finite set of values that the i th component of $\nabla f(\tilde{\mathbf{x}}^{(k)})$ may assume by \mathcal{W}_i . We define $\mathcal{W}_i^* := \mathcal{W}_i \setminus \{0\}$. Note that \mathcal{W}_i^* can be empty for some entries of $\nabla f(\tilde{\mathbf{x}}^{(k)})$, but when it is empty for all i , in accordance with (14), it implies that $\nabla f(\tilde{\mathbf{x}}^{(k)}) = 0$ and GD converges to the optimal point. Before we start our analysis, we recall a basic property of conditional expectation to facilitate the further proof.

Let X, Y, Z be random variables, then we have e.g., (Steyer and Nagel, 2017, (10.40))

$$\mathbb{E}[\mathbb{E}[X \mid Y, Z] \mid Y] = \mathbb{E}[X \mid Y]. \quad (33)$$

Moreover, for technical reasons, we introduce the quantity

$$\theta_k := \min_{i=1, \dots, n} \min_{\nabla f(\tilde{\mathbf{x}}^{(k)})_i \in \mathcal{W}_i^*} \frac{2|\nabla f(\tilde{\mathbf{x}}^{(k)})_i| - Lu}{|\nabla f(\tilde{\mathbf{x}}^{(k)})_i|}, \quad \text{where } 2 - L \leq \theta_k < 2. \quad (34)$$

The equality is approximately equal to 2 when the gradient is large compared to Lu , which is typically the case at the beginning of the process. Only when the gradient gets close to 0 and $L > 2$, θ_k may be negative. We now provide some results about the expected monotonicity and convergence rate of GD for the iteration steps under the mild constraint $\theta_k \geq 0$. We begin with the monotonicity when using SR.

Proposition 13 *Under Universal Assumptions, after k iteration steps of GD in fixed-precision arithmetic with a fixed stepsize $t < \frac{1}{L}$, suppose that the condition of Case II has been satisfied throughout the k iteration steps. If σ_1 and σ_2 in (5) are obtained by SR and $\theta_k \geq 0$ then*

$$\mathbb{E}[f(\tilde{\mathbf{x}}^{(k)})] \leq \mathbb{E}[f(\tilde{\mathbf{x}}^{(k-1)})].$$

Proof The Lipschitz gradient property (1), rephrased in terms of expectations, yields

$$\mathbb{E}[f(\tilde{\mathbf{x}}^{(k+1)})] \leq \mathbb{E}[f(\tilde{\mathbf{x}}^{(k)})] - \sum_{i=1}^n \mathbb{E}[\nabla f(\tilde{\mathbf{x}}^{(k)})_i d_i^{(k)} - \frac{1}{2} L (d_i^{(k)})^2]. \quad (35)$$

According to (33), we have

$$\mathbb{E}[\nabla f(\tilde{\mathbf{x}}^{(k)})_i \sigma_{2,i}^{(k)} \mid \nabla f(\tilde{\mathbf{x}}^{(k)})_i] = \mathbb{E}[\mathbb{E}[\nabla f(\tilde{\mathbf{x}}^{(k)})_i \sigma_{2,i}^{(k)} \mid \nabla f(\tilde{\mathbf{x}}^{(k)})_i, \sigma_{1,i}^{(k)}] \mid \nabla f(\tilde{\mathbf{x}}^{(k)})_i] = 0.$$

Therefore, letting q vary over \mathcal{W}_i^* , the set of all the possible values of $\nabla f(\tilde{\mathbf{x}}^{(k)})_i$, and utilizing the law of total expectation, we have

$$\begin{aligned} & \mathbb{E}[\nabla f(\tilde{\mathbf{x}}^{(k)})_i d_i^{(k)}] \\ &= \sum_{q \in \mathcal{W}_i^*} \mathbb{E}[\nabla f(\tilde{\mathbf{x}}^{(k)})_i d_i^{(k)} \mid \nabla f(\tilde{\mathbf{x}}^{(k)})_i = q] P(\nabla f(\tilde{\mathbf{x}}^{(k)})_i = q) \\ &= \sum_{q \in \mathcal{W}_i^*} \mathbb{E}[\nabla f(\tilde{\mathbf{x}}^{(k)})_i (t \nabla f(\tilde{\mathbf{x}}^{(k)})_i + t \sigma_{1,i}^{(k)}) \mid \nabla f(\tilde{\mathbf{x}}^{(k)})_i = q] P(\nabla f(\tilde{\mathbf{x}}^{(k)})_i = q). \end{aligned} \quad (36)$$

Similarly, we have

$$\mathbb{E}[(d_i^{(k)})^2] = \sum_{q \in \mathcal{W}_i^*} \mathbb{E}[(d_i^{(k)})^2 \mid \nabla f(\tilde{\mathbf{x}}^{(k)})_i = q] P(\nabla f(\tilde{\mathbf{x}}^{(k)})_i = q).$$

Based on (20), when $\nabla f(\tilde{\mathbf{x}}^{(k)})_i + \sigma_{1,i}^{(k)} > 0$, we have

$$(d_i^{(k)})^2 = \text{SR}(t \nabla f(\tilde{\mathbf{x}}^{(k)})_i + t \sigma_{1,i}^{(k)})^2 = \begin{cases} 0, & \text{with probability } p_0(t \nabla f(\tilde{\mathbf{x}}^{(k)})_i + t \sigma_{1,i}^{(k)}), \\ u^2, & \text{with probability } 1 - p_0(t \nabla f(\tilde{\mathbf{x}}^{(k)})_i + t \sigma_{1,i}^{(k)}). \end{cases}$$

Replacing x by $t \nabla f(\tilde{\mathbf{x}}^{(k)})_i + t \sigma_{1,i}^{(k)}$ in (7), we have

$$\mathbb{E}[d_i^{(k)} \mid \nabla f(\tilde{\mathbf{x}}^{(k)})_i, \sigma_{1,i}^{(k)}] = t \nabla f(\tilde{\mathbf{x}}^{(k)})_i + t \sigma_{1,i}^{(k)} = u(1 - p_0(t \nabla f(\tilde{\mathbf{x}}^{(k)})_i + t \sigma_{1,i}^{(k)})),$$

so that

$$\mathbb{E}[(d_i^{(k)})^2 \mid \nabla f(\tilde{\mathbf{x}}^{(k)})_i, \sigma_{1,i}^{(k)}] = u^2(1 - p_0(t \nabla f(\tilde{\mathbf{x}}^{(k)})_i + t \sigma_{1,i}^{(k)})) = u|t \nabla f(\tilde{\mathbf{x}}^{(k)})_i + t \sigma_{1,i}^{(k)}|. \quad (37)$$

It is easy to check that (37) also holds for the condition when $\nabla f(\tilde{\mathbf{x}}^{(k)})_i + \sigma_{1,i}^{(k)} < 0$. In view of (33), we have

$$\mathbb{E}[(d_i^{(k)})^2 \mid \nabla f(\tilde{\mathbf{x}}^{(k)})_i] = \mathbb{E}[\mathbb{E}[(d_i^{(k)})^2 \mid \nabla f(\tilde{\mathbf{x}}^{(k)})_i, \sigma_{1,i}^{(k)}] \mid \nabla f(\tilde{\mathbf{x}}^{(k)})_i],$$

which leads to

$$\mathbb{E}[(d_i^{(k)})^2] = \sum_{q \in \mathcal{W}_i^*} \mathbb{E}[|t \nabla f(\tilde{\mathbf{x}}^{(k)})_i + t \sigma_{1,i}^{(k)}| u \mid \nabla f(\tilde{\mathbf{x}}^{(k)})_i = q] P(\nabla f(\tilde{\mathbf{x}}^{(k)})_i = q).$$

Equation (14) implies that

$$\nabla f(\tilde{\mathbf{x}}^{(k)})_i (t \nabla f(\tilde{\mathbf{x}}^{(k)})_i + t \sigma_{1,i}^{(k)}) = |\nabla f(\tilde{\mathbf{x}}^{(k)})_i| |t \nabla f(\tilde{\mathbf{x}}^{(k)})_i + t \sigma_{1,i}^{(k)}|,$$

and together with (36), it yields

$$\begin{aligned} & \mathbb{E}[\nabla f(\tilde{\mathbf{x}}^{(k)})_i d_i^{(k)} - \frac{1}{2} L (d_i^{(k)})^2] \\ &= \sum_{q \in \mathcal{W}_i^*} \mathbb{E}[|t \nabla f(\tilde{\mathbf{x}}^{(k)})_i + t \sigma_{1,i}^{(k)}| (|\nabla f(\tilde{\mathbf{x}}^{(k)})_i| - \frac{1}{2} L u) \mid \nabla f(\tilde{\mathbf{x}}^{(k)})_i = q] P(\nabla f(\tilde{\mathbf{x}}^{(k)})_i = q). \end{aligned} \quad (38)$$

Finally, we observe that $\nabla f(\tilde{\mathbf{x}}^{(k)})_i \in \mathcal{W}_i^*$ implies $\nabla f(\tilde{\mathbf{x}}^{(k)})_i \neq 0$, and also $\theta_k \geq 0$ implies $\mathbb{E}[\nabla f(\tilde{\mathbf{x}}^{(k)})_i d_i^{(k)} - \frac{1}{2} L (d_i^{(k)})^2] \geq 0$, $i = 1, \dots, n$, which together with (35) implies that $\mathbb{E}[f(\tilde{\mathbf{x}}^{(k)})] \geq \mathbb{E}[f(\tilde{\mathbf{x}}^{(k+1)})]$. \blacksquare

Concerning the convergence rate obtained with SR, we prove the following bound.

Proposition 14 *Under the same assumptions of Proposition 13, if $\theta_j \geq 0$, $j = 0, \dots, k-1$, then*

$$\mathbb{E} [f(\tilde{\mathbf{x}}^{(k)}) - f^*] \lesssim \prod_{j=0}^{k-1} (1 - t\mu\theta_j) \cdot (f(\mathbf{x}^{(0)}) - f^*), \quad (39)$$

where $0 < 1 - t\mu\theta_j < 1$.

Proof On the basis of (34) and (38), we have

$$\begin{aligned} & \mathbb{E} [\nabla f(\tilde{\mathbf{x}}^{(k)})_i d_i^{(k)} - \frac{1}{2} L (d_i^{(k)})^2] \\ & \geq \frac{1}{2} \theta_k \sum_{q \in \mathcal{W}_i^*} \mathbb{E} [(t \nabla f(\tilde{\mathbf{x}}^{(k)})_i + t \sigma_{1,i}^{(k)}) \nabla f(\tilde{\mathbf{x}}^{(k)})_i \mid \nabla f(\tilde{\mathbf{x}}^{(k)})_i = q] P(\nabla f(\tilde{\mathbf{x}}^{(k)})_i = q) \\ & = \frac{1}{2} \theta_k t \mathbb{E} [\nabla f(\tilde{\mathbf{x}}^{(k)})_i^2 + \nabla f(\tilde{\mathbf{x}}^{(k)})_i \sigma_{1,i}^{(k)}] \\ & \stackrel{\text{Lemma 6}}{\simeq} \frac{1}{2} \theta_k t \mathbb{E} [\nabla f(\tilde{\mathbf{x}}^{(k)})_i^2]. \end{aligned} \quad (40)$$

Substituting it into (35), we obtain

$$\begin{aligned} \mathbb{E} [f(\tilde{\mathbf{x}}^{(k+1)})] & \lesssim \mathbb{E} [f(\tilde{\mathbf{x}}^{(k)})] - \sum_{i=1}^n \frac{1}{2} \theta_k t \mathbb{E} [\nabla f(\tilde{\mathbf{x}}^{(k)})_i^2] \\ & = \mathbb{E} [f(\tilde{\mathbf{x}}^{(k)})] - \frac{1}{2} \theta_k t \mathbb{E} [\|\nabla f(\tilde{\mathbf{x}}^{(k)})\|^2]. \end{aligned}$$

Substituting (32) into it, we get

$$\mathbb{E} [f(\tilde{\mathbf{x}}^{(k+1)}) - f^*] \lesssim (1 - t\mu\theta_k) \mathbb{E} [f(\tilde{\mathbf{x}}^{(k)}) - f^*].$$

Expanding the recursion, we obtain (39). Since $\theta_j, t, \mu > 0$ we have $1 - t\mu\theta_j < 1$. Finally, $\theta_j < 2$ and $t < \frac{1}{L} \leq \frac{1}{2\mu}$ imply $1 - t\mu\theta_j > 0$. \blacksquare

Looking at (39), we see that larger values of θ_j lead to tighter bounds for the expected convergence rate of GD. Comparing (4) and (39), when $\theta_j > 1$ for many iteration steps j , it is likely to achieve a stricter bound than the one available for exact arithmetic; on the contrary, when $\theta_j < 1$ for many indices j we probably get a larger bound. Next we prove that under the same condition as Proposition 13, the monotonicity of GD is also guaranteed when employing SR_ε for σ_2 .

Proposition 15 *Under the same assumptions of Proposition 13, but instead of using SR now σ_2 is obtained using SR_ε , if $\theta_k \geq 0$ in (34) then*

$$\mathbb{E} [f(\tilde{\mathbf{x}}^{(k)})] \leq \mathbb{E} [f(\tilde{\mathbf{x}}^{(k-1)})].$$

Proof Denote by \mathcal{S} the finite set of values that may be taken by $t(\nabla f(\tilde{\mathbf{x}}^{(k)})_i + \sigma_{1,i}^{(k)})$. Let \mathcal{S}_1 indicate the subset of values of \mathcal{S} such that $0 < p_\varepsilon(t(\nabla f(\tilde{\mathbf{x}}^{(k)})_i + \sigma_{1,i}^{(k)})) < 1$. Analogously, we define the subsets \mathcal{S}_2 and \mathcal{S}_3 corresponding to the conditions $p_\varepsilon = 0$ and $p_\varepsilon = 1$, respectively. Finally, we introduce the quantity

$$\omega_i^{(k)} := u^{-1}(u - |t(\nabla f(\tilde{\mathbf{x}}^{(k)})_i + \sigma_{1,i}^{(k)})|).$$

Note that the numerator of $\omega_i^{(k)}$ indicates the distance of $t(\nabla f(\tilde{\mathbf{x}}^{(k)})_i + \sigma_{1,i}^{(k)})$ to u and $-u$ for $t(\nabla f(\tilde{\mathbf{x}}^{(k)})_i + \sigma_{i,1}^{(k)}) \in \mathcal{S}_2$ and $t(\nabla f(\tilde{\mathbf{x}}^{(k)})_i + \sigma_{i,1}^{(k)}) \in \mathcal{S}_3$, respectively. According to the definition of SR_ε , see (8b), when $p_\varepsilon(t \nabla f(\tilde{\mathbf{x}}^{(k)})_i + t \sigma_{1,i}^{(k)})$ equals 0 or 1 it follows that $\omega_i^{(k)} < \varepsilon$. Further, since $t(\nabla f(\tilde{\mathbf{x}}^{(k)})_i + \sigma_{i,1}^{(k)}) \in \mathcal{S}_2$ and $t(\nabla f(\tilde{\mathbf{x}}^{(k)})_i + \sigma_{i,1}^{(k)}) \in \mathcal{S}_3$ are mutually exclusive events, we have $P(t(\nabla f(\tilde{\mathbf{x}}^{(k)})_i + \sigma_{1,i}^{(k)}) \in \{\mathcal{S}_2 \cup \mathcal{S}_3\}) = P(t(\nabla f(\tilde{\mathbf{x}}^{(k)})_i + \sigma_{1,i}^{(k)}) \in \mathcal{S}_2) + P(t(\nabla f(\tilde{\mathbf{x}}^{(k)})_i + \sigma_{1,i}^{(k)}) \in \mathcal{S}_3)$. Therefore, we define the real-valued function h as the map that associates with the random variable $\nabla f(\tilde{\mathbf{x}}^{(k)})_i + \sigma_{1,i}^{(k)}$ and the quantity:

$$h(\nabla f(\tilde{\mathbf{x}}^{(k)})_i + \sigma_{1,i}^{(k)}) := \varepsilon P(t(\nabla f(\tilde{\mathbf{x}}^{(k)})_i + \sigma_{1,i}^{(k)}) \in \mathcal{S}_1) + \omega_i^{(k)} P(t(\nabla f(\tilde{\mathbf{x}}^{(k)})_i + \sigma_{1,i}^{(k)}) \in \{\mathcal{S}_2 \cup \mathcal{S}_3\}). \quad (41)$$

When $\nabla f(\tilde{\mathbf{x}}^{(k)})_i + \sigma_{1,i}^{(k)}$ is not identically zero random variable, we have

$$\begin{aligned} \mathbb{E}[\sigma_{2,i}^{(k)} \mid \nabla f(\tilde{\mathbf{x}}^{(k)})_i, \sigma_{1,i}^{(k)}] &= u \operatorname{sign}(\nabla f(\tilde{\mathbf{x}}^{(k)})_i) (\varepsilon P(t(\nabla f(\tilde{\mathbf{x}}^{(k)})_i + \sigma_{1,i}^{(k)}) \in \mathcal{S}_1) \\ &\quad + \omega_i^{(k)} u P(t(\nabla f(\tilde{\mathbf{x}}^{(k)})_i + \sigma_{1,i}^{(k)}) \in \{\mathcal{S}_2 \cup \mathcal{S}_3\})) \\ &= u \operatorname{sign}(\nabla f(\tilde{\mathbf{x}}^{(k)})_i) h(\nabla f(\tilde{\mathbf{x}}^{(k)})_i + \sigma_{1,i}^{(k)}). \end{aligned}$$

Proceeding analogously as for (36), we obtain

$$\begin{aligned} \mathbb{E}[\nabla f(\tilde{\mathbf{x}}^{(k)})_i d_i^{(k)}] & \quad (42) \\ &= \sum_{q \in \mathcal{W}_i^*} \mathbb{E}[\nabla f(\tilde{\mathbf{x}}^{(k)})_i (t \nabla f(\tilde{\mathbf{x}}^{(k)})_i + t \sigma_{1,i}^{(k)}) \mid \nabla f(\tilde{\mathbf{x}}^{(k)})_i = q] P(\nabla f(\tilde{\mathbf{x}}^{(k)})_i = q) \\ &\quad + \sum_{q \in \mathcal{W}_i^*} \mathbb{E}[u |\nabla f(\tilde{\mathbf{x}}^{(k)})_i| h(\nabla f(\tilde{\mathbf{x}}^{(k)})_i + \sigma_{1,i}^{(k)}) \mid \nabla f(\tilde{\mathbf{x}}^{(k)})_i = q] P(\nabla f(\tilde{\mathbf{x}}^{(k)})_i = q). \end{aligned}$$

Following a similar procedure to the one obtaining (37), with SR_ε , we have

$$\begin{aligned} \mathbb{E}[(d_i^{(k)})^2 \mid \nabla f(\tilde{\mathbf{x}}^{(k)})_i, \sigma_{1,i}^{(k)}] &= u^2 (1 - p_\varepsilon(t \nabla f(\tilde{\mathbf{x}}^{(k)})_i + t \sigma_{1,i}^{(k)})) \\ &= (u |t \nabla f(\tilde{\mathbf{x}}^{(k)})_i + t \sigma_{1,i}^{(k)}| + \varepsilon u^2) P(\nabla f(\tilde{\mathbf{x}}^{(k)})_i + \sigma_{1,i}^{(k)} \in \mathcal{S}_1) \\ &\quad + (u |t \nabla f(\tilde{\mathbf{x}}^{(k)})_i + \sigma_{1,i}^{(k)}| + \omega_i^{(k)} u^2) P(\nabla f(\tilde{\mathbf{x}}^{(k)})_i + t \sigma_{1,i}^{(k)} \in \{\mathcal{S}_2 \cup \mathcal{S}_3\}). \\ &= u |t \nabla f(\tilde{\mathbf{x}}^{(k)})_i + t \sigma_{1,i}^{(k)}| + u^2 h(\nabla f(\tilde{\mathbf{x}}^{(k)})_i + \sigma_{1,i}^{(k)}). \end{aligned}$$

Therefore:

$$\begin{aligned} \mathbb{E}[(d_i^{(k)})^2] &= \sum_{q \in \mathcal{W}_i^*} \mathbb{E}[u |t \nabla f(\tilde{\mathbf{x}}^{(k)})_i + t \sigma_{1,i}^{(k)}| \mid \nabla f(\tilde{\mathbf{x}}^{(k)})_i = q] P(\nabla f(\tilde{\mathbf{x}}^{(k)})_i = q) \\ &\quad + \sum_{q \in \mathcal{W}_i^*} \mathbb{E}[u^2 h(\nabla f(\tilde{\mathbf{x}}^{(k)})_i + \sigma_{1,i}^{(k)}) \mid \nabla f(\tilde{\mathbf{x}}^{(k)})_i = q] P(\nabla f(\tilde{\mathbf{x}}^{(k)})_i = q). \end{aligned}$$

Together with (42) and in accordance with (33), we obtain

$$\begin{aligned}
 & \mathbb{E} \left[\nabla f(\tilde{\mathbf{x}}^{(k)})_i d_i^{(k)} - \frac{1}{2} L (d_i^{(k)})^2 \right] \\
 &= \sum_{q \in \mathcal{W}_i^*} \mathbb{E} \left[\nabla f(\tilde{\mathbf{x}}^{(k)})_i d_i^{(k)} - \frac{1}{2} L (d_i^{(k)})^2 \mid \nabla f(\tilde{\mathbf{x}}^{(k)})_i = q \right] P(\nabla f(\tilde{\mathbf{x}}^{(k)})_i = q) \\
 &= \sum_{q \in \mathcal{W}_i^*} \mathbb{E} \left[|t \nabla f(\tilde{\mathbf{x}}^{(k)})_i + t \sigma_{1,i}^{(k)}| (|\nabla f(\tilde{\mathbf{x}}^{(k)})_i| - \frac{1}{2} L u) \mid \nabla f(\tilde{\mathbf{x}}^{(k)})_i = q \right] P(\nabla f(\tilde{\mathbf{x}}^{(k)})_i = q) \\
 &+ \sum_{q \in \mathcal{W}_i^*} \mathbb{E} \left[(u |\nabla f(\tilde{\mathbf{x}}^{(k)})_i| - \frac{1}{2} L u^2) h(\nabla f(\tilde{\mathbf{x}}^{(k)})_i + \sigma_{1,i}^{(k)}) \mid \nabla f(\tilde{\mathbf{x}}^{(k)})_i = q \right] P(\nabla f(\tilde{\mathbf{x}}^{(k)})_i = q).
 \end{aligned} \tag{43}$$

When $\theta_k \geq 0$, it follows that $\mathbb{E} \left[\nabla f(\tilde{\mathbf{x}}^{(k)})_i d_i^{(k)} - \frac{1}{2} L (d_i^{(k)})^2 \right] \geq 0$, which implies $\mathbb{E} [f(\tilde{\mathbf{x}}^{(k)})] \leq \mathbb{E} [f(\tilde{\mathbf{x}}^{(k-1)})]$. \blacksquare

Proposition 15 shows that under the same conditions as in Proposition 13, the monotonicity of GD can be also obtained by applying SR_ε . Further, we show that a stricter bound on convergence can be realized by utilizing SR_ε compared to that of SR. First let us define (cf. (41))

$$\beta_k := \min_{i=1, \dots, n} h(\nabla f(\tilde{\mathbf{x}}^{(k)})_i + \sigma_{1,i}^{(k)}),$$

where $\beta_k \leq \varepsilon$ for all k and define

$$\tau_2 := \min_{j=0, \dots, k} \frac{\beta_j u \mathbb{E} [\|\nabla f(\tilde{\mathbf{x}}^{(j)})\|]}{\mathbb{E} [\|\nabla f(\tilde{\mathbf{x}}^{(j)})\|^2]}. \tag{44}$$

When $\theta_k \geq 0$ in (34), it implies that $\mathbb{E} [\|\nabla f(\tilde{\mathbf{x}}^{(k)})\|] \geq \frac{1}{2} L u$. On the basis of Jensen's inequality, we get

$$\tau_2 \leq \frac{2\beta_j}{L} \underset{L t \leq 1}{\leq} 2t\beta_j \leq 2t\varepsilon, \quad \text{for all } j = 1, \dots, k.$$

With (44), we may achieve a stricter bound on the convergence of GD.

Proposition 16 *Under the same assumption of Proposition 15 but instead of $t \leq \frac{1}{L}$ we have $t \leq \frac{1}{(1+2\varepsilon)L}$, if $\theta_j \geq 0$ in (34) for all j , then with $0 < \tau_2 \leq 2t\varepsilon$ we have*

$$\mathbb{E} [f(\tilde{\mathbf{x}}^{(k)}) - f^*] \lesssim \prod_{j=0}^{k-1} (1 - (t + \tau_2) \mu \theta_j) \cdot (f(\mathbf{x}^{(0)}) - f^*), \tag{45}$$

where $0 < (t + \tau_2) \mu \theta_j < 1$.

Proof Substituting θ_k (cf. (34)) and β_k into (43), we get

$$\begin{aligned}
 & \mathbb{E} [\nabla f(\tilde{\mathbf{x}}^{(k)})_i d_i^{(k)} - \frac{1}{2} L (d_i^{(k)})^2] \\
 & \geq \frac{1}{2} \theta_k \sum_{q \in \mathcal{W}_i^*} \mathbb{E} [(t \nabla f(\tilde{\mathbf{x}}^{(k)})_i + t \sigma_{1,i}^{(k)}) \nabla f(\tilde{\mathbf{x}}^{(k)})_i \mid \nabla f(\tilde{\mathbf{x}}^{(k)})_i = q] P(\nabla f(\tilde{\mathbf{x}}^{(k)})_i = q) \\
 & \quad + \frac{1}{2} \theta_k \sum_{q \in \mathcal{W}_i^*} \mathbb{E} [\beta_k |\nabla f(\tilde{\mathbf{x}}^{(k)})_i| u \mid \nabla f(\tilde{\mathbf{x}}^{(k)})_i = q] P(\nabla f(\tilde{\mathbf{x}}^{(k)})_i = q) \\
 & = \frac{1}{2} \theta_k \mathbb{E} [t \nabla f(\tilde{\mathbf{x}}^{(k)})_i^2 + t \nabla f(\tilde{\mathbf{x}}^{(k)})_i \sigma_{1,i}^{(k)} + \beta_k u |\nabla f(\tilde{\mathbf{x}}^{(k)})_i|] \\
 & \simeq \frac{1}{2} \theta_k (t \mathbb{E} [\nabla f(\tilde{\mathbf{x}}^{(k)})_i^2] + \beta_k u \mathbb{E} [|\nabla f(\tilde{\mathbf{x}}^{(k)})_i|]), \quad \text{from Lemma 6.} \tag{46}
 \end{aligned}$$

Substituting it into (35), we obtain

$$\begin{aligned}
 \mathbb{E} [f(\tilde{\mathbf{x}}^{(k+1)})] & \lesssim \mathbb{E} [f(\tilde{\mathbf{x}}^{(k)})] - \sum_{i=1}^n \frac{1}{2} \theta_k t \mathbb{E} [\nabla f(\tilde{\mathbf{x}}^{(k)})_i^2] - \sum_{i=1}^n \frac{1}{2} \theta_k \beta_k u \mathbb{E} [|\nabla f(\tilde{\mathbf{x}}^{(k)})_i|] \\
 & \leq \mathbb{E} [f(\tilde{\mathbf{x}}^{(k)})] - \frac{1}{2} \theta_k (t \mathbb{E} [\|\nabla f(\tilde{\mathbf{x}}^{(k)})\|^2] + \beta_k u \mathbb{E} [\|\nabla f(\tilde{\mathbf{x}}^{(k)})\|_1]) \\
 & \leq \mathbb{E} [f(\tilde{\mathbf{x}}^{(k)})] - \frac{1}{2} \theta_k (t \mathbb{E} [\|\nabla f(\tilde{\mathbf{x}}^{(k)})\|^2] + \beta_k u \mathbb{E} [\|\nabla f(\tilde{\mathbf{x}}^{(k)})\|]). \tag{47}
 \end{aligned}$$

In accordance with Jensen's inequality, we have

$$\tau_2 \leq \frac{\beta_k u \mathbb{E} [\|\nabla f(\tilde{\mathbf{x}}^{(k)})\|]}{\mathbb{E} [\|\nabla f(\tilde{\mathbf{x}}^{(k)})\|^2]} \leq \frac{\beta_k u \mathbb{E} [\|\nabla f(\tilde{\mathbf{x}}^{(k)})\|]}{\mathbb{E} [\|\nabla f(\tilde{\mathbf{x}}^{(k)})\|]^2} = \frac{\beta_k u}{\mathbb{E} [\|\nabla f(\tilde{\mathbf{x}}^{(k)})\|]}.$$

Substituting (44) into (47), we obtain

$$\mathbb{E} [f(\tilde{\mathbf{x}}^{(k+1)})] \lesssim \mathbb{E} [f(\tilde{\mathbf{x}}^{(k)})] - \frac{1}{2} \theta_k (t + \tau_2) \mathbb{E} [\|\nabla f(\tilde{\mathbf{x}}^{(k)})\|^2].$$

Substituting (32) into the right-hand side and expanding the recursion k times, we obtain the desired result with $0 < \tau_2 \leq 2t\varepsilon$. Furthermore, on the basis of definition of SR_ε that $0 < \varepsilon < 1$ and the property $\theta_k < 2$, it is easy to check that $0 < (t + \tau_2) \mu \theta_j < 1$, which concludes the proof. \blacksquare

In general, a larger ε in SR_ε (cf. Section 2.2) allows for larger values of β_j and of τ_2 . Comparing (39) and (45), a larger value of τ_2 leads to a stricter bound on the convergence rate. Under the same condition as the one to SR , utilizing SR_ε to evaluate $\sigma_2^{(k)}$ may achieve faster convergence than the one gained by SR . In the next section, we analyze the convergence behavior of GD for Case III.

4.2.3 CASE III

In this case, we consider updating rules satisfying (21), for which the updating vector are comprised of entries $d_i^{(k)}$ that satisfy either (18) or (20). We show that the convergence rate is bounded by a value that is larger than the bound in Case I and smaller than the bound in Case II.

For the next result, we need to introduce the following quantity:

$$\alpha_k := \frac{\sum c_2 t (\theta_k - 1) \mathbb{E} [\nabla f(\tilde{\mathbf{x}}^{(k)})_i^2]}{\mathbb{E} [\|\nabla f(\tilde{\mathbf{x}}^{(k)})\|^2]}, \tag{48}$$

where \mathcal{C}_2 is the set defined in the condition of Case III. It is easy to see that $|\alpha_k| \leq t|\theta_k - 1|$. When $0 \leq \theta_k < 2$ (cf. (34)), then $-t \leq \alpha_k < t$. Informally, α_k tends to be positive when the gradient is large (in the beginning of the process), and negative when the gradient is close to 0. This α_k occurs in the upper bound of the next proposition. To let the result be meaningful (that is, to ensure decrease of the expected function value), we need an upper bound on α_k .

Proposition 17 *Under Universal Assumptions and the condition of Case III (17), suppose that both σ_1 and σ_2 in (5) are obtained using SR with fixed stepsize t such that $t < \frac{1}{4L}$. If $\theta_j \geq 0$ in (34) for all j , then we have*

$$\mathbb{E}[f(\tilde{\mathbf{x}}^{(k)}) - f^*] \lesssim \prod_{j=0}^{k-1} (1 - \mu(t + \alpha_j)) \cdot (f(\mathbf{x}^{(0)}) - f^*), \quad (49)$$

where α_j is from (48) and $0 < \mu(t + \alpha_j) < 1$.

Proof Because of (21), we have

$$\begin{aligned} \mathbb{E}[f(\tilde{\mathbf{x}}^{(k+1)})] &\leq \mathbb{E}[f(\tilde{\mathbf{x}}^{(k)})] - \mathbb{E}[\nabla f(\tilde{\mathbf{x}}^{(k)})^T \mathbf{d}^{(k)}] + \frac{1}{2} L \mathbb{E}[\|\mathbf{d}^{(k)}\|^2] \\ &= \mathbb{E}[f(\tilde{\mathbf{x}}^{(k)})] - \sum_{i \in \mathcal{C}_1 \cup \mathcal{C}_2} \mathbb{E}[t \nabla f(\tilde{\mathbf{x}}^{(k)})_i^2 + t \nabla f(\tilde{\mathbf{x}}^{(k)})_i \sigma_{1,i}^{(k)} + \nabla f(\tilde{\mathbf{x}}^{(k)})_i \sigma_{2,i}^{(k)} - \frac{1}{2} L (d_i^{(k)})^2]. \end{aligned} \quad (50)$$

When SR is used to evaluate $\sigma_{1,i}^{(k)}$ and $\sigma_{2,i}^{(k)}$, on the basis of (30) and (40), we have

$$\begin{aligned} \mathbb{E}[f(\tilde{\mathbf{x}}^{(k+1)})] &\lesssim \mathbb{E}[f(\tilde{\mathbf{x}}^{(k)})] - \sum_{i \in \mathcal{C}_1} \frac{1}{2} t \mathbb{E}[\nabla f(\tilde{\mathbf{x}}^{(k)})_i^2] - \sum_{i \in \mathcal{C}_2} \frac{1}{2} \theta_k t \mathbb{E}[\nabla f(\tilde{\mathbf{x}}^{(k)})_i^2] \\ &= \mathbb{E}[f(\tilde{\mathbf{x}}^{(k)})] - \sum_{i=1}^n \frac{1}{2} t \mathbb{E}[\nabla f(\tilde{\mathbf{x}}^{(k)})_i^2] - \sum_{i \in \mathcal{C}_2} (\frac{1}{2} \theta_k - \frac{1}{2}) t \mathbb{E}[\nabla f(\tilde{\mathbf{x}}^{(k)})_i^2] \\ &= \mathbb{E}[f(\tilde{\mathbf{x}}^{(k)})] - \frac{1}{2} t \mathbb{E}[\|\nabla f(\tilde{\mathbf{x}}^{(k)})\|^2] - \sum_{i \in \mathcal{C}_2} \frac{1}{2} t (\theta_k - 1) \mathbb{E}[\nabla f(\tilde{\mathbf{x}}^{(k)})_i^2]. \end{aligned} \quad (51)$$

Substituting (48) into (51) and expanding the recursion k times, we obtain (49). The properties $t < \frac{1}{4L} \leq \frac{1}{2\mu}$ and $0 \leq \theta_j < 2$ imply that $1 - 2\mu t > 0$ and $-t \leq \alpha_j < t$, which indicate that $1 - \mu(t + \alpha_j) > 1 - 2\mu t > 0$. \blacksquare

Equation (51) can be seen as the combination of (31) with $\rho_k = 0$ and (40). From (51), it can be seen that when $0 \leq \theta_k < 2$, we obtain monotonicity on the objective function. When $\theta_k = 1$, we may achieve similar convergence to Case I, i.e.,

$$\mathbb{E}[f(\tilde{\mathbf{x}}^{(k+1)})] \lesssim \mathbb{E}[f(\tilde{\mathbf{x}}^{(k)})] - \frac{1}{2} t \mathbb{E}[\|\nabla f(\tilde{\mathbf{x}}^{(k)})\|^2],$$

which leads to the same convergence bound as in Corollary 12, i.e.,

$$\mathbb{E}[f(\tilde{\mathbf{x}}^{(k)}) - f^*] \lesssim (1 - t\mu)^k (f(\mathbf{x}^{(0)}) - f^*).$$

However, when $0 < \theta_k < 1$, we may obtain a negative α_k in (49), which implies a larger bound on the convergence rate than Case I. In particular, the convergence rate of (49)

depends on the number of $d_i^{(k)} \in \mathcal{C}_2$. When $0 < \theta_k < 1$ a larger number of $d_i^{(k)} \in \mathcal{C}_2$ causes smaller value of α_k (cf. (48)). On the contrary, when $\theta_k \geq 1$ a larger number of $d_i^{(k)} \in \mathcal{C}_2$ results in larger value of α_k . When many $d_i^{(k)}$ belong to \mathcal{C}_2 and the components of the gradient vectors are close to zero (α_k is negative), we may achieve a slower convergence.

Next, we show that with SR_ε we may obtain a stricter bound on the convergence rate than that obtained by SR (cf. (49)).

Proposition 18 *Under Universal Assumptions and the condition of Case III (17), suppose that σ_1 and σ_2 in (5) are obtained using SR and SR_ε , respectively, with fixed stepsize t such that $t < \frac{1}{4L}$. If $\theta_j \geq 0$ in (34) for all j and with α_j from (48), then there exists $0 < \tau_2 \leq 2t\varepsilon$ such that*

$$\mathbb{E}[f(\tilde{\mathbf{x}}^{(k)}) - f^*] \lesssim \prod_{j=0}^{k-1} (1 - \mu(t + \alpha_j + \theta_j \tau_2)) \cdot (f(\mathbf{x}^{(0)}) - f^*). \quad (52)$$

Proof When $\sigma_{1,i}^{(k)}$ and $\sigma_{2,i}^{(k)}$ are evaluated by SR and SR_ε , respectively, substituting (30) and (46) into (50) yields

$$\begin{aligned} \mathbb{E}[f(\tilde{\mathbf{x}}^{(k+1)})] &\lesssim \mathbb{E}[f(\tilde{\mathbf{x}}^{(k)})] - \frac{1}{2} \sum_{i \in \mathcal{C}_1} (t \mathbb{E}[\nabla f(\tilde{\mathbf{x}}^{(k)})_i^2] + \mathbb{E}[\sigma_{2,i}^k \nabla f(\tilde{\mathbf{x}}^{(k)})_i]) \\ &\quad - \frac{1}{2} \theta_k \sum_{i \in \mathcal{C}_2} (t \mathbb{E}[\nabla f(\tilde{\mathbf{x}}^{(k)})_i^2] + \beta_k u \mathbb{E}[|\nabla f(\tilde{\mathbf{x}}^{(k)})_i|]) \\ &= \mathbb{E}[f(\tilde{\mathbf{x}}^{(k)})] - \frac{1}{2} t \mathbb{E}[\|\nabla f(\tilde{\mathbf{x}}^{(k)})\|^2] \\ &\quad - \sum_{i \in \mathcal{C}_1} (\mathbb{E}[\sigma_{2,i}^k \nabla f(\tilde{\mathbf{x}}^{(k)})_i] - \frac{1}{2} \theta_k \beta_k u \mathbb{E}[|\nabla f(\tilde{\mathbf{x}}^{(k)})_i|]) \\ &\quad - \sum_{i \in \mathcal{C}_2} \frac{1}{2} (\theta_k - 1) t \mathbb{E}[\nabla f(\tilde{\mathbf{x}}^{(k)})_i^2] - \frac{1}{2} \theta_k \beta_k u \mathbb{E}[\|\nabla f(\tilde{\mathbf{x}}^{(k)})\|]. \end{aligned}$$

Furthermore, the properties $\beta_k u \leq |\mathbb{E}[\sigma_{2,i}^{(k)}]|$ and $\theta_k \leq 2$ imply that $\frac{1}{2} \beta_k u \mathbb{E}[|\nabla f(\tilde{\mathbf{x}}^{(k)})_i|] \leq \mathbb{E}[\sigma_{2,i}^k \nabla f(\tilde{\mathbf{x}}^{(k)})_i]$. On the basis of (44) and (48), we have

$$\mathbb{E}[f(\tilde{\mathbf{x}}^{(k+1)})] \lesssim \mathbb{E}[f(\tilde{\mathbf{x}}^{(k)})] - \frac{1}{2} (t + \theta_k \tau_2 + \alpha_k) \mathbb{E}[\|\nabla f(\tilde{\mathbf{x}}^{(k)})\|^2].$$

Expanding the recursion k times, we obtain (52), with $\tau_2 \leq 2t\varepsilon$ and $|\alpha_j| < t|\theta_j - 1|$ for all j . Since $\mu(t + \alpha_j + \theta_j \tau_2) \leq \mu t(1 + |\theta_j - 1| + 2\theta_j t\varepsilon) \leq \mu t(1 + 1 + 4\varepsilon) \leq 2\mu t(1 + 2\varepsilon) \leq Lt(1 + 2\varepsilon) \leq \frac{1+2\varepsilon}{4} < 1$. Further the property $1 - 2\mu t > 0$ and $-t \leq \alpha_j < t$ indicate that $1 - \mu(t + \alpha_j) > 1 - 2\mu t > 0$, combining with the property $\theta_j \tau_2 \geq 0$ we have $0 \leq \mu(t + \alpha_j + \theta_j \tau_2) < 1$. \blacksquare

Again, with SR_ε , we obtain a stricter bound on the convergence rate than that obtained by SR under Case III (comparing (49) and (52)), which shows that a faster convergence may be obtained when using SR_ε in place of SR for σ_2 . Equation (52) shows that the convergence bound obtained by SR_ε is determined by the value of ε and t , where a faster convergence can be obtained by choosing a larger ε in SR_ε or a larger t .

In the next section, we compare our convergence analysis of GD using fixed-point arithmetic to the one using floating-point arithmetic.

5. Comparison with floating-point arithmetic

In this section, we show that our rounding method SR_ε works differently in fixed-point arithmetic and floating-point arithmetic. Using SR_ε to implement GD in fixed-point arithmetic, the rounding bias on each entry of iterate is in the same scale (u). However, owing to the fact that numbers in IEEE floating-point numbers are not uniformly distributed, the same holds the rounding bias on each entry of iterate. In particular, when implementing GD with limited-precision in floating-point arithmetic, using SR_ε , the updating stepsize is adaptive to the entries of each iterate.

Now let us dive into the difference between fixed-point and floating-point computation for different rounding methods. We start by comparing their expressions of the updating vector $\mathbf{d}^{(k)}$ of GD in fixed-point and floating-point number formats. In accordance with the argument in (Xia et al., 2022, Sec. 4.2) that the small numbers can be represented by the subnormal numbers in floating-point number formats, therefore stagnation of GD happens when evaluating the subtraction in (3). However, the stagnation of GD happens when evaluating the multiplication of t and gradients in fixed-point number formats. To have a clear observation, we assume that stagnation starts from k th iteration step and all the computations before stagnation are exact (errors are negligible) for both fixed-point and floating-point arithmetic, i.e., $\text{fi}(\nabla f(\mathbf{x}^{(k)})) = \nabla f(\mathbf{x}^{(k)})$ and $\text{fl}(t \text{fl}(\nabla f(\mathbf{x}^{(k)}))) = t \nabla f(\mathbf{x}^{(k)})$ for fixed-point and floating-point arithmetic, where $\text{fl}(\cdot)$ denotes a general rounding operator that convert a real number $x \in \mathbb{R}$ to the floating-point number representation \hat{x} .

When GD stagnates with RN for the i th coordinate of $\mathbf{x}^{(k)}$ and $d_i^{(k)} \neq 0$, we have a fixed magnitude of $d_i^{(k)}$ using stochastic rounding methods for fixed-point number representation, given by

$$d_i^{(k)} = u \text{sign}(\nabla f(\mathbf{x}^{(k)})_i).$$

Under the same assumption, we have an adaptive magnitude of $d_i^{(k)}$ using stochastic rounding methods for floating-point number representation. On the grounds of the model of floating-point operation (Higham, 2002, (2.4)), we have the following value for $d_i^{(k)}$

$$d_i^{(k)} = \begin{cases} \text{sign}(\nabla f(\mathbf{x}^{(k)})_i) |x_i^{(k)}| \delta_i^{(k)} + t \nabla f(\mathbf{x}^{(k)})_i (1 - \delta_i^{(k)}), & \text{if } \text{sign}(x_i^{(k)} \nabla f(\mathbf{x}^{(k)})_i) = 1, \\ \text{sign}(\nabla f(\mathbf{x}^{(k)})_i) |x_i^{(k)}| \delta_i^{(k)} + t \nabla f(\mathbf{x}^{(k)})_i (1 + \delta_i^{(k)}), & \text{if } \text{sign}(x_i^{(k)} \nabla f(\mathbf{x}^{(k)})_i) = -1, \end{cases} \quad (53)$$

where $0 < \delta_i^{(k)} < 2u$ denotes the relative error caused by evaluating $x_i^{(k)} - t \nabla f(\mathbf{x}^{(k)})_i$ using stochastic rounding methods. For different stochastic rounding methods, $d_i^{(k)}$ may be either zero or one of the expressions in (53) with different probability distributions. Therefore, GD behaves differently with different rounding methods and number representations.

Now let us study the difference between different rounding methods in each number representation. For fixed-point arithmetic, we obtain the following updating vectors of GD when using SR and SR_ε .

Proposition 19 *Assume the use of fixed-point arithmetic to implement GD, and that $\text{RN}(d_i^{(k)}) = 0$ for the i th component in $\mathbf{d}^{(k)}$, i.e., $|t \nabla f(\mathbf{x}^{(k)})_i| < \frac{1}{2}u$. If $\text{fi}(\nabla f(\mathbf{x}^{(k)})) =$*

$\nabla f(\mathbf{x}^{(k)})$, then for SR we have

$$\mathbb{E}[d_i^{(k)} \mid t \nabla f(\tilde{\mathbf{x}}^{(k)})_i] = t \nabla f(\tilde{\mathbf{x}}^{(k)})_i. \quad (54)$$

For SR_ε we have

$$\mathbb{E}[d_i^{(k)} \mid t \nabla f(\mathbf{x}^{(k)})_i] = \begin{cases} u \text{sign}(\nabla f(\mathbf{x}^{(k)})_i), & \text{if } \varepsilon \geq 1 - \frac{|t \nabla f(\mathbf{x}^{(k)})_i|}{u}, \\ t \nabla f(\mathbf{x}^{(k)})_i + \varepsilon u \text{sign}(\nabla f(\mathbf{x}^{(k)})_i), & \text{otherwise.} \end{cases}$$

Proof The unbiased property of SR yields (54). According to (8a) and (54), for $\nabla f(\mathbf{x}^{(k)})_i < 0$, we have $-u p_0(t \nabla f(\mathbf{x}^{(k)})_i) = t \nabla f(\mathbf{x}^{(k)})_i$, which indicates

$$\begin{aligned} -u p_\varepsilon(t \nabla f(\mathbf{x}^{(k)})_i) &= -u (p_0(t \nabla f(\mathbf{x}^{(k)})_i) + \text{sign}(\nabla f(\mathbf{x}^{(k)})_i) \varepsilon) \\ &= t \nabla f(\mathbf{x}^{(k)})_i + \varepsilon u \text{sign}(\nabla f(\mathbf{x}^{(k)})_i). \end{aligned}$$

The same result can be obtained for $\nabla f(\mathbf{x}^{(k)})_i > 0$ by using the property $t \nabla f(\mathbf{x}^{(k)})_i = u(1 - p_0(t \nabla f(\tilde{\mathbf{x}}^{(k)})_i))$. \blacksquare

From Proposition 19, we can observe that SR and SR_ε lead to an average updating magnitude of GD that is similar to and slightly larger than the one in exact computation, respectively. The updating length of GD is independent of its iterate $\mathbf{x}^{(k)}$ in fixed-point arithmetic for both SR and SR_ε , and the rounding bias introduced by SR_ε is only dependent on u and has the same sign vector as its gradient.

For floating-point arithmetic, when GD stagnates with RN, we obtain the properties of the updating magnitudes of GD when using SR and signed- SR_ε . Note that signed- SR_ε and SR_ε have the same performance under fixed-point arithmetic. In floating-point, signed- SR_ε and SR_ε generate the same magnitude of rounding bias but the rounding bias may have different sign.

Proposition 20 *Assume the use of floating-point arithmetic to implement GD, and that $\text{RN}(x_i^{(k)} - d_i^{(k)}) = x_i^{(k)}$, i.e., $|\frac{t \nabla f(\mathbf{x}^{(k)})_i}{\tilde{x}^{(k)}}| < u$. If $\text{fl}(t \text{fl}(\nabla f(\mathbf{x}^{(k)}))) = t \nabla f(\mathbf{x}^{(k)})$, then for SR we have*

$$\mathbb{E}[d_i^{(k)} \mid x_i^{(k)} - t \nabla f(\mathbf{x}^{(k)})_i] = t \nabla f(\tilde{\mathbf{x}}^{(k)})_i. \quad (55)$$

For signed- SR_ε , when $0 < \tilde{p}_\varepsilon < 1$, we have

$$\begin{aligned} \mathbb{E}[d_i^{(k)} \mid x_i^{(k)} - t \nabla f(\mathbf{x}^{(k)})_i] & \\ = \begin{cases} (1 + \varepsilon + \varepsilon \delta_i^{(k)}) t \nabla f(\mathbf{x}^{(k)})_i + \text{sign}(\nabla f(\mathbf{x}^{(k)})_i) |x_i^{(k)}| \varepsilon \delta_i^{(k)}, & \text{if } \text{sign}(x_i^{(k)} \nabla f(\mathbf{x}^{(k)})_i) = -1, \\ (1 + \varepsilon - \varepsilon \delta_i^{(k)}) t \nabla f(\mathbf{x}^{(k)})_i + \text{sign}(\nabla f(\mathbf{x}^{(k)})_i) |x_i^{(k)}| \varepsilon \delta_i^{(k)}, & \text{if } \text{sign}(x_i^{(k)} \nabla f(\mathbf{x}^{(k)})_i) = 1, \end{cases} \end{aligned} \quad (56)$$

where $0 < \delta_i^{(k)} < 2u$.

Proof Derived from the model of floating-point number representation we have

$$\text{fl}(x_i^{(k)} - t \nabla f(\mathbf{x}^{(k)})_i) = \begin{cases} (x_i^{(k)} - t \nabla f(\mathbf{x}^{(k)})_i) (1 + \delta_i^{(k)}), & \text{if } \text{sign}(x_i^{(k)} \nabla f(\mathbf{x}^{(k)})_i) = -1, \\ (x_i^{(k)} - t \nabla f(\mathbf{x}^{(k)})_i) (1 - \delta_i^{(k)}), & \text{if } \text{sign}(x_i^{(k)} \nabla f(\mathbf{x}^{(k)})_i) = 1, \end{cases}$$

where $0 < \delta_i^{(k)} < 2u$. In light of (13), we obtain

$$\begin{aligned} d_i^{(k)} &= x_i^{(k)} - \text{fl}(x_i^{(k)} - t \nabla f(\mathbf{x}^{(k)})_i) \\ &= \begin{cases} -\delta_i^{(k)} x_i^{(k)} + t \nabla f(\mathbf{x}^{(k)})_i (1 + \delta_i^{(k)}), & \text{if } \text{sign}(x_i^{(k)} \nabla f(\mathbf{x}^{(k)})_i) = -1, \\ \delta_i^{(k)} x_i^{(k)} + t \nabla f(\mathbf{x}^{(k)})_i (1 - \delta_i^{(k)}), & \text{if } \text{sign}(x_i^{(k)} \nabla f(\mathbf{x}^{(k)})_i) = 1. \end{cases} \end{aligned}$$

Due to the zero rounding bias property of SR and taking the expectation of $d_i^{(k)}$, we obtain $\mathbb{E}[d_i^{(k)} \mid x_i^{(k)} - t \nabla f(\mathbf{x}^{(k)})_i] = t \nabla f(\mathbf{x}^{(k)})_i$, which gives (55). On the basis of (55) and (9), by making $\text{sign}(v) = \text{sign}(\nabla f(\mathbf{x}^{(k)})_i)$ in signed-SR $_\varepsilon$ (cf. (9)), when $x_i^{(k)} > 0$ and $\nabla f(\tilde{\mathbf{x}}^{(k)})_i < 0$, we have

$$\begin{aligned} \mathbb{E}[d_i^{(k)} \mid x_i^{(k)} - t \nabla f(\mathbf{x}^{(k)})_i] &= (-\delta_i^{(k)} x_i^{(k)} + t \nabla f(\mathbf{x}^{(k)})_i (1 + \delta_i^{(k)})) (1 - p_0(x_i^{(k)} - t \nabla f(\mathbf{x}^{(k)})_i) - \text{sign}(\nabla f(\mathbf{x}^{(k)})_i) \varepsilon) \\ &= t \nabla f(\mathbf{x}^{(k)})_i + \varepsilon (-\delta_i^{(k)} x_i^{(k)} + t \nabla f(\mathbf{x}^{(k)})_i (1 + \delta_i^{(k)})) \\ &= (1 + \varepsilon + \varepsilon \delta_i^{(k)}) t \nabla f(\mathbf{x}^{(k)})_i + \text{sign}(\nabla f(\mathbf{x}^{(k)})_i) |x_i^{(k)}| \varepsilon \delta_i^{(k)}. \end{aligned}$$

Analogously, when $x_i^{(k)} < 0$ and $\nabla f(\mathbf{x}^{(k)})_i > 0$, we have

$$\begin{aligned} \mathbb{E}[d_i^{(k)} \mid x_i^{(k)} - t \nabla f(\mathbf{x}^{(k)})_i] &= (-\delta_i^{(k)} x_i^{(k)} + t \nabla f(\mathbf{x}^{(k)})_i (1 + \delta_i^{(k)})) (p_0(x_i^{(k)} - t \nabla f(\mathbf{x}^{(k)})_i) + \text{sign}(\nabla f(\mathbf{x}^{(k)})_i) \varepsilon) \\ &= (1 + \varepsilon + \varepsilon \delta_i^{(k)}) t \nabla f(\mathbf{x}^{(k)})_i + \text{sign}(\nabla f(\mathbf{x}^{(k)})_i) |x_i^{(k)}| \varepsilon \delta_i^{(k)}. \end{aligned}$$

Therefore, (56) holds for the case when $\text{sign}(x_i^{(k)} \nabla f(\mathbf{x}^{(k)})_i) = -1$. The proof of (56) for the case $\text{sign}(x_i^{(k)} \nabla f(\mathbf{x}^{(k)})_i) = 1$ can be obtained by an analogous argument as the one for $\text{sign}(x_i^{(k)} \nabla f(\mathbf{x}^{(k)})_i) = -1$. \blacksquare

Since $t \nabla f(\mathbf{x}^{(k)})_i$ is relatively small compared to $x_i^{(k)}$ in Proposition 20, $|x_i^{(k)}|$ has a significant impact on the magnitude of $d_i^{(k)}$. Consequently, $\mathbb{E}[d_i^{(k)} \mid x_i^{(k)} - t \nabla f(\mathbf{x}^{(k)})_i]$ is automatically adaptive to the scale of $x_i^{(k)}$ for each entry of $\mathbf{x}^{(k)}$ by using signed-SR $_\varepsilon$ in floating-point arithmetic, but it does not hold for SR. Comparing Proposition 19 and Proposition 20, the magnitude of the updating vector of GD is independent of u or the current iterate when using SR in both fixed-point and floating-point arithmetic. In particular, when GD stagnates with RN, SR may lead to a similar convergence behavior to exact computation on average, that is with uniform stepsize t for each entry of $\mathbf{x}^{(k)}$. However, when using signed-SR $_\varepsilon$, the convergence speed mainly depends on the magnitude of the iterate of GD in floating-point arithmetic and is largely improved by the adaptive rounding bias along each coordinate of $\mathbf{x}^{(k)}$, while the updating magnitude of GD is almost consistent along each coordinate of $\mathbf{x}^{(k)}$ in fixed-point number representation.

In general, SR performs similarly in both floating-point and fixed-point arithmetic; SR $_\varepsilon$ and signed-SR $_\varepsilon$ have a better effect than SR on both floating-point and fixed-point arithmetic. Thanks to the non-uniform distributed number representation in floating-point arithmetic, the rounding bias caused by SR $_\varepsilon$ and signed-SR $_\varepsilon$ is also non-uniform, which

results in a faster convergence than that of GD in exact arithmetic. For fixed-point arithmetic, the rounding bias caused by SR_ϵ is also uniform as its number distribution, which may have a less obvious advantage in accelerating GD than in floating-point arithmetic. Though, floating-point number representation has a wider number representation owing to the non-uniform distributed number representation, many practical low-cost embedded microprocessors and microcontrollers (e.g., FPGA designs) are limited to finite-precision signal processing using fixed-point arithmetic due to the cost and complexity of floating point hardware. In both number arithmetic, SR_ϵ outperforms SR in implementing GD.

6. Simulation studies

In this section, we validate our theoretical results by applying GD with limited-precision number formats on several case studies: a quadratic problem, the two-dimensional Rosenbrock’s function, Himmelblau’s function, a binary logistic regression model (BLR), and a four-layer fully connected NN. We numerically show that Rosenbrock’s function satisfies the PL inequality in a certain domain and reaches a linear convergence of GD. Himmelblau’s function is used to demonstrate that GD with stochastic rounding techniques can converge exactly to the optimal point instead of just a neighborhood of around it. BLR is proven to satisfy the PL condition by Karimi et al. (2016), we validate our theoretical results by training a BLR using different rounding methods and learning rates. Finally, we study the convergence of GD on training a four-layer NN and show that though the four-layer NN does not satisfy the PL condition, the simulation results are similar to those of functions that satisfy the PL condition.

As discussed in Section 3.3, the stagnation of GD is normally caused by σ_2 in (5). Therefore, for each of the simulation study, we employ two different number formats for evaluating σ_2 and for working precision (implementing all the other operations in this working precision). Note that, in all case studies, apart from the four-layer NN, we use low-precision fixed-point number formats, whose implementation rely on the Matlab fi toolbox. Due to the slow computation speed of fi toolbox, in the four-layer NN case, we only evaluate σ_2 with limited-precision fixed-point numbers and use single-precision computations for the other operations. Note that, selecting the best number format for a procedure that rely on fixed-point arithmetic operations is problem dependent and, to the authors’ knowledge, there is no systemic way to select the priori best number format for a given problem. In the preprocessing procedure, we test various values for QI and QF in different case studies. The values of the QI are chosen to avoid overflow problems in each case study. The considered values for QF is taken as large as possible in such a way that it allows us to easily observe the influence of rounding errors and validate our theoretical results: we start by setting u to 2^{-12} , and then we increase or decrease u until the largest value that guarantees the convergence. The considered number formats is summerized in Table 2.

For the cases of Rosenbrock’s function and NN, we also compare the performances of low-precision fixed-point computation with those of low-precision floating-point computation. For all the simulation studies, we compare the results obtained by SR and SR_ϵ to those obtained with RN. The baselines are obtained by single-precision (Binary32) floating-point computation with RN. We remark that, there is a huge difference between the magnitude of the machine precision of single precision (2^{-23}) and those of other fixed-point number

Table 2: Number formats of fixed-point representation for different case studies. The third column indicates how the multiplication $t \nabla f(\mathbf{x}_k)$ is carried out.

Case study	Working precision	Multiplication
Quadratic	Q26.6	Q26.6
Rosenbrock	Q6.10	Q10.6
Himmelblau	Q8.8	Q8.8
BLR	Q15.8	Q15.8 and Q15.6
Four-layer NN	Binary32	Q8.8

formats, that stay above 2^{-10} . Therefore, we look at the comparison with the baselines as a surrogate of a comparison with exact arithmetic.

6.1 Quadratic problem

In Section 5, we have demonstrated that SR performs very similarly in fixed-point and floating-point arithmetic, yet signed- SR_ϵ and SR_ϵ have a clearly positive impact on floating-point arithmetic and a modestly positive impact on fixed-point arithmetic. To better understand this phenomenon, let us compare the convergence behavior of GD using different rounding methods with fixed-point and floating-point arithmetic. For instance, when optimizing a least square problem of the form $F_1(\mathbf{x}) = \frac{1}{2}(\mathbf{x} - \mathbf{x}^*)^T A (\mathbf{x} - \mathbf{x}^*)$, where $A = \text{diag}(100, 10, 10^{-3}, 10^{-3}, 10^{-3})$ and $\mathbf{x}^* = [10^{-1}, 1, 10, 100, 1000]^T$, so that the entries of \mathbf{x}^* are of different scales. When using fixed-point arithmetic, the rounding bias introduced by SR_ϵ can not take care of the scale of each entry of \mathbf{x}^* , but it can be done when using SR_ϵ in floating-point arithmetic. To achieve a descent updating direction, we employ signed- SR_ϵ (Xia et al., 2022, Def. 2.3) in floating-point arithmetic to customize the sign of the rounding bias.

Fig. 2 shows the comparison of objective values when optimizing F_1 using GD with different rounding schemes using fixed-point arithmetic (Fig. 2a) and floating-point arithmetic (Fig. 2b). Due to the overlapping between the results of SR and Binary32, we utilize a dashed-line for SR (only) in Fig. 2 for the readability. For both figures, the baseline is obtained by optimizing F_1 using single-precision (32-bit) computation and RN. In Fig. 2a, both σ_1 and σ_2 are obtained using the same rounding scheme. For instance, the yellow line in Fig. 2a shows that both σ_1 and σ_2 are obtained using RN using fixed-point number representation Q26.6. In Fig. 2b, we apply 8-bit floating-point computation with 3 significant bits. Comparing figures 2a and 2b, it can be observed that the convergence rates of GD using RN and SR are very similar in fixed-point and floating-point number formats. However, SR_ϵ performs extraordinarily different in these two number formats. It suggests that the accumulated rounding bias in the descent direction in fixed-point arithmetic maintains a linear convergence rate but with a smaller base than the one obtained by the exact computation, while an almost superlinear convergence rate seems to be obtained using SR_ϵ in floating-point arithmetic.

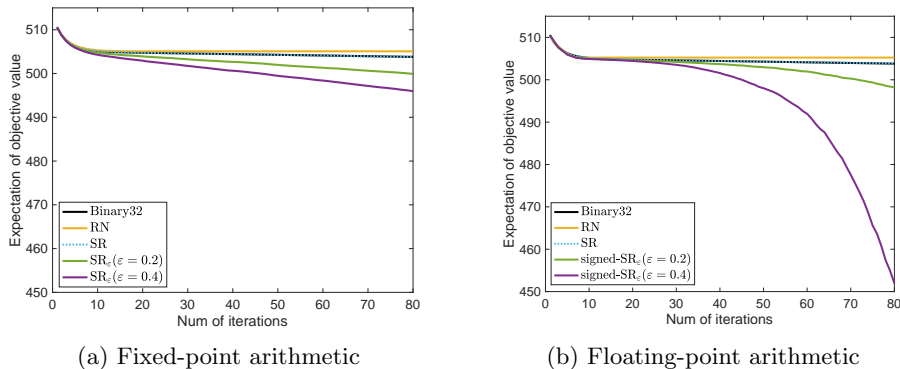


Figure 2: A least square problem: comparison of the objective values using different rounding scheme with fixed-point arithmetic (Q26.6) (a) and floating-point arithmetic (8 bits with 3 significant bits) (b); settings: rate $t = 2^{-6}$ and $\mathbf{x}^* = [10^{-1}, 1, 10, 100, 1000]^T \in \mathbb{R}^5$.

6.2 Rosenbrock’s function

Rosenbrock function is a non-convex function, characterized by a wide almost flat valley around its optimum; it is defined as $F_2(\mathbf{x}) = (1 - x_1)^2 + 100(x_2 - x_1^2)^2$. Although it does not satisfy (2) for all \mathbf{x} , it can be numerically checked that the Rosenbrock’s function satisfies (1) and (2) with $L = 2610$ and $\mu = 0.2$ for $\mathbf{x} \in [0, 2]^2$.

Fig. 3 shows the trajectories (Fig. 3a) and the corresponding means of objective function evaluations over 30 simulations (Fig. 3b) when implementing GD with fixed-point numbers formats and different rounding schemes. To better observe the influence of rounding errors on the convergence of GD, we apply low precision to compute the multiplication of t and the gradients (Q10.6) and a higher precision for the remaining operations to maintain the accuracy (Q6.10). The starting point is $\mathbf{x}^{(0)} = [0, 0]^T$. It can be seen from Fig. 3a that GD relying on RN stagnates quite early because of the loss of gradient information. SR follows a very similar convergence to the baseline that validates Corollary 12. When using SR_ε , a larger ε leads to a faster convergence to the optimum, that matches the conclusion in Theorem 11, Proposition 16, and Proposition 18. Furthermore, from Fig. 3b, with $\varepsilon = 0.4$, the mean of the objective value at the 64th iteration is similar to the one obtained with single-precision at the 400th iteration, i.e., 0.31. Due to the wide valley in Rosenbrock’s function, a small deviation causes a large oscillation in the objective function. Therefore, the small rounding bias introduced by SR_ε will introduce some oscillations in the objective function’s values.

Further, we repeat the same simulation study with 8-bit floating-point number format with 3 significant digits. Fig. 4 shows the trajectories and the corresponding mean of objective function evaluations for using different rounding methods in floating-point arithmetic. Note that signed- SR_ε introduces rounding biases with same magnitudes as those obtained by SR_ε . From Fig. 4, it can be observed that RN causes stagnation of GD, and SR follows a similar trajectory to the one by single-precision computation. Signed- SR_ε significantly

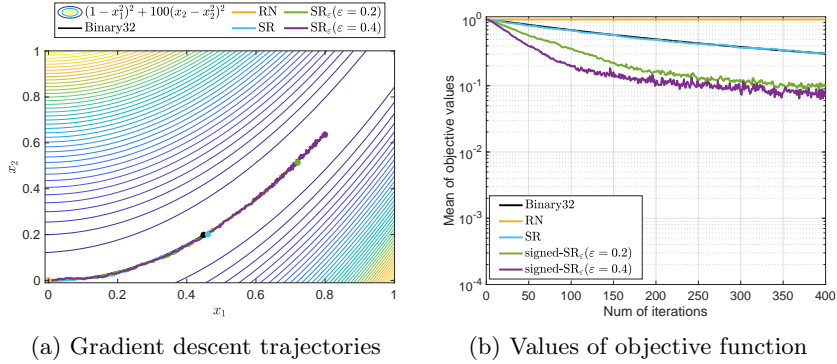


Figure 3: Rosenbrock’s function in two dimensions: comparison of the gradient descent trajectories (a) and of the correspondent objective values (b); settings: rate $t = 2^{-10}$ and Q10.6 for evaluating the multiplication of t and gradient and Q6.10 for the remaining operations.

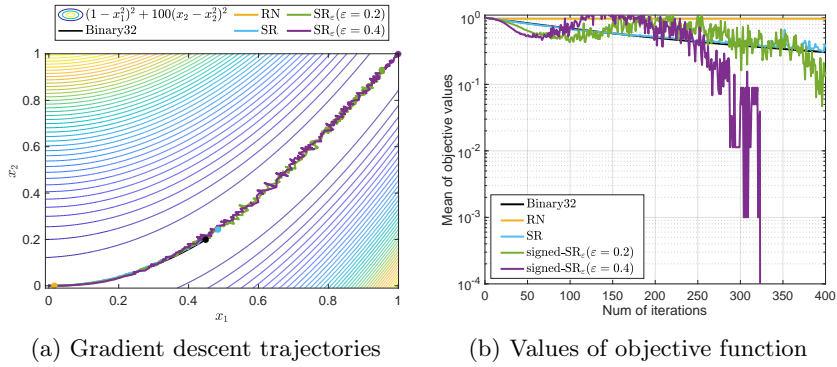


Figure 4: Rosenbrock’s function in two dimensions: comparison of the gradient descent trajectories (a) and of the correspondent objective values (b); settings: rate $t = 2^{-10}$ and Binary8 (Xia et al., 2022, Sec. 2.1) with 3 significant bits.

accelerates the convergence of GD owing to the rounding bias in the descent direction. When $\varepsilon = 0.4$, although the mean of objective function values suffers from oscillations, GD converges to the optimum with 324 maximum iterations for all 30 simulations.

6.3 Himmelblau’s function

Now, in line with the discussion in Section 3.1, we show with an illustrative example that when the optimal point \mathbf{x}^* can be represented exactly in the available number format, we have that $\|\tilde{\mathbf{x}}^{(k)} - \mathbf{x}^*\| \rightarrow 0$. On the other hand, when \mathbf{x}^* cannot be represented exactly, GD converges to the border of a neighborhood of \mathbf{x}^* whose size depends on u . Let us consider the minimization of the Himmelblau’s function $F_3(\mathbf{x}) = (x_1^2 + x_2 - 11)^2 + (x_1 + x_2^2 - 7)^2$, using single-precision computation and fixed-point number representation with Q8.8. We

remark that Himmelblau’s function does not satisfy the PL condition for all x , but this is inconsequential for this test. The function f has four global minimizers \mathbf{x}_i^* , for $i = 1, \dots, 4$, known in closed form. In particular, we focus on the case where GD converges towards $\mathbf{x}_1^* = [3, 2]^T$, that is exactly representable, and when it converges to $\mathbf{x}_4^* = [3.584428, -1.848126]^T$ that is not. In Fig. 5 we report the averaged objective function values (over 30 runs) as the rounding scheme is chosen among RN, SR, and SR_ϵ . As anticipated, when GD converges to $\mathbf{x}_1^* = [3, 2]^T$, all the stochastic rounding methods retrieves the exact value \mathbf{x}_1^* , while RN makes GD to stagnate due to the vanishing gradient problem. When the starting point is close to $\mathbf{x}_4^* = [3.584428, -1.848126]^T$, all the rounding methods can only guide GD to a neighborhood around \mathbf{x}_4^* .

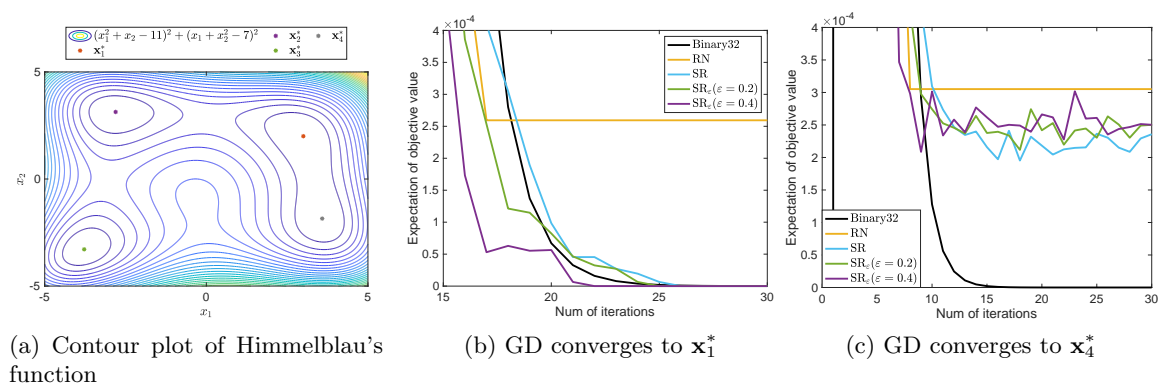


Figure 5: Himmelblau’s Function: contour plot with the 4 global minimizers \mathbf{x}_i^* , with $i = 1, \dots, 4$ (a), comparison of the objective values when GD converges to \mathbf{x}_1^* (b) and comparison of the objective values when GD converges to \mathbf{x}_4^* (c); with stepsize $t = 0.012$ and fixed-point numbers Q8.8.

6.4 Binary logistic regression

Let us study the influence of rounding errors on solving logistic regression problems. Logistic regression is a statistic model that predicts the probability of a class or event that will happen. It is commonly used to solve binary classification problems and is proven to satisfy the PL condition by Karimi et al. (2016) over any compact set. We use BLR to classify the handwritten digits 3 and 8 in the MNIST database. As in Gupta et al. (2015), the pixel values are normalized to $[0, 1]$. The default decision threshold is set for interpreting probabilities to class labels, that is 0.5, since the sample class sizes are almost equal Chen et al. (2006). Specifically, class 1 is defined for those predicted scores larger than or equal to 0.5.

We study the convergence of GD with different rounding precisions. For each simulation study, we demonstrate two rounding precisions, i.e., the working precision and the precision for evaluating σ_2 . Fig. 6 shows the comparison of the BLR’s testing errors, obtained with the various rounding methods. In Fig. 6a, we employ enough digits (Q15.8) so that GD has no stagnation utilizing RN. It can be observed that SR and RN lead to very similar

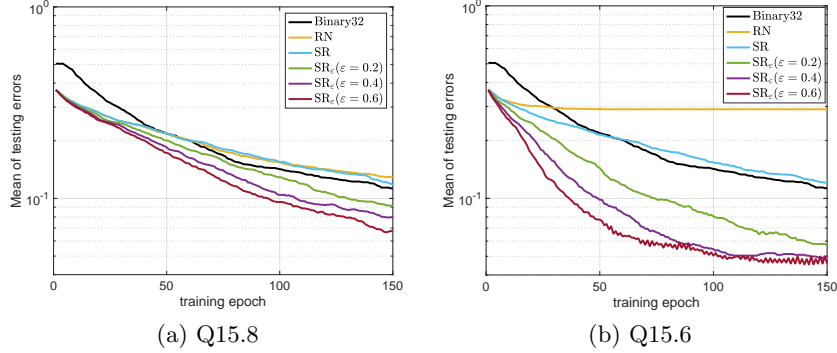


Figure 6: Mean of objective values over 10 simulations of BLR with stepsize $t = 0.1$ between RN, SR and SR_ϵ with $\epsilon = 0.2$, $\epsilon = 0.4$ and $\epsilon = 0.6$ with working precision Q15.8 and the precision for evaluating σ_2 , i.e., Q15.8 (a) and Q15.6 (b).

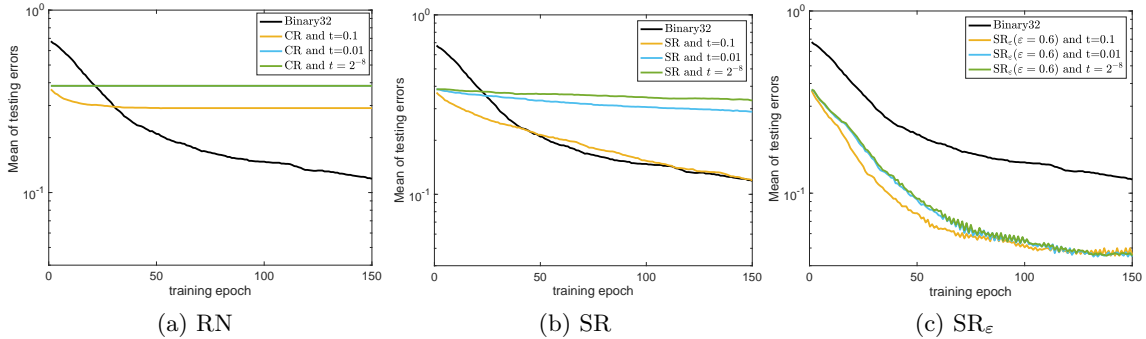


Figure 7: Mean of objective values over 10 simulations with working precision Q15.8, precision for evaluating σ_2 Q15.6, and different stepsize 0.1, 0.01 and the smallest number that can be represented in Q15.8, i.e, $2^{-8} \approx 0.004$, for RN (a), SR (b), and SR_ϵ (c).

results, while SR_ϵ ends in a faster convergence of GD than that of RN and SR with the same rounding precision. Further, a larger ϵ produces a faster convergence of GD. Keeping the same working precision and lowering the precision in evaluating σ_2 , we observe the stagnation of GD with RN and that SR provides a very similar result to the one in Fig. 6a; see Fig. 6b. In the same figure, SR_ϵ makes use of the large rounding errors and produces a much faster convergence rate of GD than the one in Fig. 6a. Again, a faster convergence of GD can be obtained by utilizing a larger ϵ . However, comparing Fig. 6a and Fig. 6b, it can be observed that when the rounding precision and ϵ are both large, oscillations may happen when GD converges closer to the global optimum; see the result of SR_ϵ with $\epsilon = 0.6$ in Fig. 6b.

Next, we study the influence of the stepsize t in (5) on the convergence of GD with low-precision computation for different rounding methods. We employ the same number

format as in Fig. 6b and we vary the stepsize of GD. In particular, we consider $t = 0.1$, 0.01 and the smallest number that can be represented in Q15.8, i.e., $2^{-8} \approx 0.004$ for each rounding method such as RN, SR, and SR_ε with $\varepsilon = 0.6$. Fig. 7 shows the results obtained using the different values of t and rounding schemes. From Fig. 7a, it can be seen that a smaller t causes GD stagnate earlier with RN. When SR is employed (cf. Fig. 7a), the convergence rate is significantly more sensitive to the value of t . With employment of SR, a small t leads to a slower convergence rate. When t is relatively small, e.g., $t = 2^{-8}$, GD almost stagnates with SR; see Fig. 7b. However, it can be observed that the convergence rate obtained using SR_ε is hardly affected by the stepsize when $t \leq 0.1$. In general, both RN and SR are sensitive to t , while SR_ε is less sensitive to t due to the parameter ε in (8a). When t is small, the probability of rounding numbers towards 0 in SR (cf. (7)) is close to 1, while it is dominated by $1 - \varepsilon$ in SR_ε (cf. (8a)). Therefore, an almost constant rounding probability is achieved in SR_ε , that makes SR_ε less sensitive to t when implementing GD in a low-precision number format.

6.5 Four-layer fully connected NN

Now we show that our theoretical conclusion for problems satisfying the PL condition is also applicable for the training of a four-layer fully connected NN, i.e., the convergence rate of GD with SR_ε is faster than the one with SR, though the PL condition does not hold here. The NN is trained to classify the 10 handwritten digits (from 0 to 9) in the MNIST database. Again, the pixel values are normalized to $[0, 1]$. The NN is built with the ReLu activation function in the hidden layer and the softmax activation function in the output layer. The hidden layers contain 512, 256, and 128 units. In the backward propagation, the cross-entropy loss function is optimized using the gradient descent method. The weights matrix is initialized using Xavier initialization (Glorot and Bengio, 2010) and the bias is initialized as a zero vector.

Fig. 8a shows the means of testing error of the NNs trained using Binary32 for working precision and Q8.8 for evaluating σ_2 with different rounding methods, such as RN, SR, and SR_ε . Again, RN causes the stagnation of GD due to the vanishing gradient problems. SR results in a very similar testing error to single-precision computation. The testing error is around 0.06 with 400 iterations of GD with SR and single-precision computation, while a similar level accuracy can be achieved by SR_ε with around 150 iterations. Comparing the results of SR_ε with $\varepsilon = 0.2$ and $\varepsilon = 0.4$, larger oscillations are gained with larger ε . Overall, SR_ε with $\varepsilon = 0.2$ leads to a slightly lower testing error than SR_ε with $\varepsilon = 0.4$. Next, we repeat the simulations with 16-bit floating-point number format with 5 significant digits using different rounding methods. From Fig. 8b, it can be seen that the results are very similar to that of fixed-point number formats. Comparing Fig. 8a and Fig. 8b, The results of SR_ε with floating-point number format is slightly better than that of fixed-point number format, but it can be almost negligible.

In general, when convergence is guaranteed, low-precision computation can result in a faster convergence rate compared to higher precision when employing GD using SR_ε ; see Fig. 3, Fig. 6, and Fig. 8. With low-precision computation, SR leads to very similar results of GD to the exact computation, while RN may cause GD stagnate. SR is sensitive to the stepsize of GD such that it may suffer from loss of gradients as RN or very slow convergence,

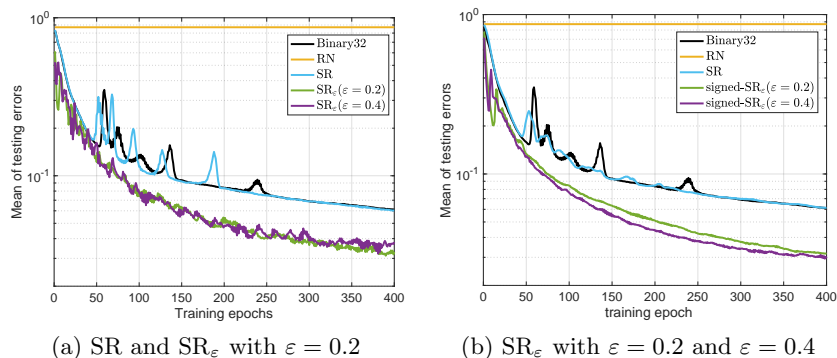


Figure 8: Mean of testing errors of the NN trained over 10 simulations using fixed-point number format Q8.8 (a) and using Binary16 with 5 significant digits (b).

when the gradients and the stepsize are too small or when the rounding precision is too large; see e.g., Fig. 7b. SR_ϵ is less sensitive to the stepsize of GD such that changing t can hardly affect the convergence rate of GD; see Fig. 7c. However, when computing GD using SR_ϵ method with large ϵ , oscillation may happen. When comparing the effects of rounding bias in fixed-point and floating-point arithmetic, SR_ϵ with low-precision floating-point computation behaves like a gradient descent method with adaptive stepsizes in each coordinate of the current iterate, whereas SR_ϵ with low-precision fixed-point computation performs similarly to a strategy that combines vanilla gradient descent and stochastic sign gradient descent method. For most of the numerical studies, SR_ϵ causes a faster convergence of GD in floating-point arithmetic than in fixed-point arithmetic; nevertheless, when training a fully connected NN the convergence of GD with SR_ϵ in fixed-point arithmetic is fairly similar to that in floating-point arithmetic.

7. Conclusion

We have studied the convergence of the gradient descent method (GD) in limited-precision fixed-point arithmetic using unbiased stochastic rounding (SR) and ϵ -biased stochastic rounding (SR_ϵ) under the Polyak–Łojasiewicz condition (PL). The influence of rounding errors on the convergence of GD are analyzed in three cases: when the updating length of GD is dominated by the magnitude of gradient vector, when it mainly depends on the rounding precision, and when both quantities play an important role.

In the analysis, we have proven that a linear convergence rate of GD can be obtained with low-precision computation by utilizing SR and SR_ϵ under the PL condition. One of the main contributions of this paper is that the convergence bound of GD with SR_ϵ is shown to be stricter than that of GD with SR for all the three cases. For instance, we have shown in Theorem 11 and Corollary 12 that in Case I, we have a linear convergence in the presence of rounding errors with factor $1 - t\mu - \tau_1$ and $1 - t\mu$ by using SR_ϵ and SR, respectively, where τ_1 is determined by the bias factor ϵ in SR_ϵ and μ is the PL constant.

With numerical studies, we have shown that SR_ε can provide a faster convergence than SR and RN on average, using the same number format. The comparison of convergence analysis between floating-point and fixed-point computation illustrates that SR_ε with low-precision floating-point computation performs similarly to a gradient descent method with adaptive stepsizes in each coordinate of the current iterate, while SR_ε with low-precision fixed-point computation behaves like a combination of vanilla gradient descent and stochastic sign gradient descent method. The numerical studies illustrate that for the training of a fully connected neural network (NN), the convergence of GD with SR_ε in fixed-point arithmetic is very similar to that in floating-point arithmetic. In both number formats, SR_ε may considerably accelerate the convergence of GD with low-precision computation, for both training of logistic regression model and NN, and this is potentially valuable for machine learning.

Acknowledgments

We thank Mark Peletier for discussions on the upper bound of the PL constant. This research was funded by the EU ECSEL Joint Undertaking under grant agreement no. 826452.

Appendix A. Proofs of Lemmas

In this appendix we prove some helpful lemmas used in our convergence analysis.

Proof of Lemma 5 When $t|\nabla f(\tilde{\mathbf{x}}^{(k)})_i + \sigma_{1,i}^{(k)}| = u$, that leads to $\sigma_{2,i}^{(k)} = 0$, condition (14) gives $-1 \leq r_i^{(k)} \leq 1$. When $t|\nabla f(\tilde{\mathbf{x}}^{(k)})_i + \sigma_{1,i}^{(k)}| > u$, observing that $\sigma_{2,i}^{(k)} \leq u$, we have $r_i^{(k)} = \frac{t\sigma_{1,i}^{(k)} + \sigma_{2,i}^{(k)}}{t\nabla f(\tilde{\mathbf{x}}^{(k)})_i} < \frac{t\sigma_{1,i}^{(k)} + t\nabla f(\tilde{\mathbf{x}}^{(k)})_i + t\sigma_{1,i}^{(k)}}{t\nabla f(\tilde{\mathbf{x}}^{(k)})_i} \leq 3$. Concerning the lower bound we consider separately the cases where $\sigma_{1,i}^{(k)}$ and $\nabla f(\tilde{\mathbf{x}}^{(k)})_i$ have the same or opposite signs. When $\text{sign}(\sigma_{1,i}) = \text{sign}(\nabla f(\tilde{\mathbf{x}}^{(k)})_i)$ we have

$$r_i^{(k)} \geq \frac{|t\sigma_{1,i}| - |\sigma_{2,i}|}{|t\nabla f(\tilde{\mathbf{x}}^{(k)})_i|} \geq \frac{|t\sigma_{1,i}| - |t\nabla f(\tilde{\mathbf{x}}^{(k)})_i + t\sigma_{1,i}|}{|t\nabla f(\tilde{\mathbf{x}}^{(k)})_i|} \geq -1.$$

When $\text{sign}(\sigma_{1,i}) = -\text{sign}(\nabla f(\tilde{\mathbf{x}}^{(k)})_i)$, (15) states that $|t\nabla f(\tilde{\mathbf{x}}^{(k)})_i| - |t\sigma_{1,i}^{(k)}| \geq u$, which implies $\frac{|t\nabla f(\tilde{\mathbf{x}}^{(k)})_i| - |t\sigma_{1,i}^{(k)}|}{|t\nabla f(\tilde{\mathbf{x}}^{(k)})_i|} \geq \frac{u}{|t\nabla f(\tilde{\mathbf{x}}^{(k)})_i|}$. Therefore, we have

$$r_i^{(k)} \geq \frac{-|t\sigma_{1,i}^{(k)}| - |\sigma_{2,i}^{(k)}|}{|t\nabla f(\tilde{\mathbf{x}}^{(k)})_i|} \geq -1 + \frac{u - |\sigma_{2,i}^{(k)}|}{|t\nabla f(\tilde{\mathbf{x}}^{(k)})_i|} \geq -1. \quad \blacksquare$$

Proof of Lemma 6 Clearly, we have

$$\mathbb{E}[\nabla f(\tilde{\mathbf{x}}^{(k)})^T (\nabla f(\tilde{\mathbf{x}}^{(k)}) + \boldsymbol{\sigma}_1^{(k)})] = \mathbb{E}[\|\nabla f(\tilde{\mathbf{x}}^{(k)})\|^2] + \sum_{i=1}^n \mathbb{E}[\sigma_{1,i}^{(k)} \nabla f(\tilde{\mathbf{x}}^{(k)})_i].$$

Universal Assumptions 2. implies $\mathbb{E}[\sigma_{1,i}^{(k)} \mid \nabla f(\tilde{\mathbf{x}}^{(k)})_i] = \mathcal{O}(u^2)$ and based on the law of total expectation, we obtain

$$\begin{aligned} \left| \mathbb{E}[\sigma_{1,i}^{(k)} \nabla f(\tilde{\mathbf{x}}^{(k)})_i] \right| &= \left| \sum_{\nabla f(\tilde{\mathbf{x}}^{(k)})_i=q} \mathbb{E}[\sigma_{1,i}^{(k)} \nabla f(\tilde{\mathbf{x}}^{(k)})_i \mid \nabla f(\tilde{\mathbf{x}}^{(k)})_i = q] P(\nabla f(\tilde{\mathbf{x}}^{(k)})_i = q) \right| \\ &\leq \sum_{\nabla f(\tilde{\mathbf{x}}^{(k)})_i=q} \mathcal{O}(u^2) |q| P(\nabla f(\tilde{\mathbf{x}}^{(k)})_i = q) \\ &= \mathcal{O}(u^2) \mathbb{E}[|\nabla f(\tilde{\mathbf{x}}^{(k)})_i|], \end{aligned}$$

which in turn yields that $\sum_{i=1}^n \mathbb{E}[\sigma_{1,i}^{(k)} \nabla f(\tilde{\mathbf{x}}^{(k)})_i]$ is bounded from above by

$$\mathcal{O}(u^2) \mathbb{E}[\|\nabla f(\tilde{\mathbf{x}}^{(k)})\|_1] \leq \sqrt{n} \mathcal{O}(u^2) \mathbb{E}[\|\nabla f(\tilde{\mathbf{x}}^{(k)})\|] \leq L_\chi \sqrt{n} \mathcal{O}(u^2). \quad \blacksquare$$

Proof of Lemma 8 When SR_ε is applied, on the basis of (6) and (8), we have

$$\begin{aligned} \mathbb{E}[\sigma_{2,i}^{(k)} \mid t(\nabla f(\tilde{\mathbf{x}}^{(k)})_i + \sigma_{1,i}^{(k)})] &= \begin{cases} \varepsilon u \text{sign}(\nabla f(\tilde{\mathbf{x}}^{(k)})_i + \sigma_{1,i}^{(k)}), & 0 < p_\varepsilon < 1, \\ [t(\nabla f(\tilde{\mathbf{x}}^{(k)})_i + \sigma_{1,i}^{(k)})] - t(\nabla f(\tilde{\mathbf{x}}^{(k)})_i + \sigma_{1,i}^{(k)}) + u, & p_\varepsilon = 0, \\ [t(\nabla f(\tilde{\mathbf{x}}^{(k)})_i + \sigma_{1,i}^{(k)})] - t(\nabla f(\tilde{\mathbf{x}}^{(k)})_i + \sigma_{1,i}^{(k)}), & p_\varepsilon = 1. \end{cases} \end{aligned} \quad (57)$$

Note that we omit the dependency on $t(\nabla f(\tilde{\mathbf{x}}^{(k)})_i + \sigma_{1,i}^{(k)})$ in p_ε for brevity. Furthermore, $p_\varepsilon(t(\nabla f(\tilde{\mathbf{x}}^{(k)})_i + \sigma_{1,i}^{(k)})) = 0$ implies $\nabla f(\tilde{\mathbf{x}}^{(k)})_i + \sigma_{1,i}^{(k)} > 0$ and $p_\varepsilon(t(\nabla f(\tilde{\mathbf{x}}^{(k)})_i + \sigma_{1,i}^{(k)})) = 1$ implies $\nabla f(\tilde{\mathbf{x}}^{(k)})_i + \sigma_{1,i}^{(k)} < 0$; on the basis of (14), we have $\text{sign}(\nabla f(\tilde{\mathbf{x}}^{(k)})_i + \sigma_{1,i}^{(k)}) = \text{sign}(\nabla f(\tilde{\mathbf{x}}^{(k)})_i)$ from which follows

$$\begin{aligned} \mathbb{E}[\sigma_{2,i}^{(k)} \nabla f(\tilde{\mathbf{x}}^{(k)})_i \mid t(\nabla f(\tilde{\mathbf{x}}^{(k)})_i + \sigma_{1,i}^{(k)})] &= \begin{cases} \varepsilon u |\nabla f(\tilde{\mathbf{x}}^{(k)})_i|, & 0 < p_\varepsilon < 1, \\ ||[t(\nabla f(\tilde{\mathbf{x}}^{(k)})_i + \sigma_{1,i}^{(k)})] - t(\nabla f(\tilde{\mathbf{x}}^{(k)})_i + \sigma_{1,i}^{(k)}) + u| |\nabla f(\tilde{\mathbf{x}}^{(k)})_i|, & p_\varepsilon = 0, \\ ||[t(\nabla f(\tilde{\mathbf{x}}^{(k)})_i + \sigma_{1,i}^{(k)})] - t(\nabla f(\tilde{\mathbf{x}}^{(k)})_i + \sigma_{1,i}^{(k)})| |\nabla f(\tilde{\mathbf{x}}^{(k)})_i|, & p_\varepsilon = 1, \end{cases} \end{aligned}$$

which are all positive random variables for all the three cases, concluding the claim. \blacksquare

Proof of Lemma 10 We denote by \mathcal{S} the finite set of values that the i th component of $\nabla f(\tilde{\mathbf{x}}^{(k)}) + \sigma_1^{(k)}$ can assume. The set \mathcal{S}_1 is the subset of \mathcal{S} such that for all $\nabla f(\tilde{\mathbf{x}}^{(k)})_i + \sigma_{1,i}^{(k)} \in \mathcal{S}_1$ satisfying $0 < p_\varepsilon(t(\nabla f(\tilde{\mathbf{x}}^{(k)})_i + \sigma_i^{(k)})) < 1$. Analogously we define \mathcal{S}_2 and \mathcal{S}_3 associated with the conditions $p_\varepsilon = 0$ and $p_\varepsilon = 1$, respectively. According to the law of total expectation, we have

$$\mathbb{E}[\sigma_{2,i}^{(k)} \nabla f(\tilde{\mathbf{x}}^{(k)})_i] = \sum_{j=1,2,3} \mathbb{E}[\sigma_{2,i}^{(k)} \nabla f(\tilde{\mathbf{x}}^{(k)})_i \mid f(\tilde{\mathbf{x}}^{(k)})_i + \sigma_i^{(k)} \in \mathcal{S}_j] P(f(\tilde{\mathbf{x}}^{(k)})_i + \sigma_i^{(k)} \in \mathcal{S}_j).$$

Note that, in view of (8b), we have

$$p_\epsilon = 1 \quad \Rightarrow \quad |[t(\nabla f(\tilde{\mathbf{x}}^{(k)})_i + \sigma_{1,i}^{(k)})] - t(\nabla f(\tilde{\mathbf{x}}^{(k)})_i + \sigma_{1,i}^{(k)})| < \epsilon u$$

and

$$p_\epsilon = 0 \quad \Rightarrow \quad |[t(\nabla f(\tilde{\mathbf{x}}^{(k)})_i + \sigma_{1,i}^{(k)})] - t(\nabla f(\tilde{\mathbf{x}}^{(k)})_i + \sigma_{1,i}^{(k)}) + u| < \epsilon u.$$

Together with (57), we obtain $\min_{i=1,\dots,n} \mathbb{E} [\sigma_{2,i}^{(k)} \nabla f(\tilde{\mathbf{x}}^{(k)})_i] \leq \epsilon u \min_{i=1,\dots,n} \mathbb{E} [|\nabla f(\tilde{\mathbf{x}}^{(k)})_i|]$. Jensen's inequality gives that $\sqrt{n} \min_{i=1,\dots,n} \mathbb{E} [|\nabla f(\tilde{\mathbf{x}}^{(k)})_i|] \leq \mathbb{E} [\|\nabla f(\tilde{\mathbf{x}}^{(k)})\|]$; together with condition (23), we have

$$\begin{aligned} \rho_k &= \min_{i=1,\dots,n} \frac{n \mathbb{E} [\sigma_{2,i}^{(k)} \nabla f(\tilde{\mathbf{x}}^{(k)})_i]}{\mathbb{E} [\|\nabla f(\tilde{\mathbf{x}}^{(k)})\|^2]} \leq \frac{n \epsilon u \min_{i=1,\dots,n} \mathbb{E} [|\nabla f(\tilde{\mathbf{x}}^{(k)})_i|]}{\mathbb{E} [\|\nabla f(\tilde{\mathbf{x}}^{(k)})\|^2]} \\ &\leq \frac{\sqrt{n} \epsilon u \mathbb{E} [\|\nabla f(\tilde{\mathbf{x}}^{(k)})\|]}{\mathbb{E} [\|\nabla f(\tilde{\mathbf{x}}^{(k)})\|^2]} \stackrel{(23)}{\leq} \frac{2t\epsilon \mathbb{E} [\|\nabla f(\tilde{\mathbf{x}}^{(k)})\|^2]}{\mathbb{E} [\|\nabla f(\tilde{\mathbf{x}}^{(k)})\|^2]}, \end{aligned}$$

which leads to $\rho_k \leq 2t\epsilon$, according to Jensen's inequality. ■

References

- F. Biagini and M. Campanino. *Elements of probability and statistics*. Springer, 2016.
- S. Boyd and L. Vandenberghe. *Convex Optimization*. Cambridge University Press, Cambridge, 2004.
- Z. Charles and D. Papailiopoulos. Stability and generalization of learning algorithms that converge to global optima. In *Int. Conf. Mach. Learn.*, pages 745–754. PMLR, 2018.
- J. Chen, C.-A. Tsai, H. Moon, H. Ahn, J. Young, and C.-H. Chen. Decision threshold adjustment in class prediction. *SAR QSAR Environ. Res.*, 17(3):337–352, 2006.
- M. P. Connolly, N. J. Higham, and T. Mary. Stochastic rounding and its probabilistic backward error analysis. *SIAM J. Sci. Comput.*, 43(1):A566–A585, 2021.
- S. Frei and Q. Gu. Proxy convexity: A unified framework for the analysis of neural networks trained by gradient descent. In *Proc. 35th Conf. Neural Inf. Process. Syst.*, pages 7937–7949, 2021.
- X. Glorot and Y. Bengio. Understanding the difficulty of training deep feedforward neural networks. In *Proc. 13th Int. Conf. Artif. Intell. Stat.*, pages 249–256, 2010.
- S. Gupta, A. Agrawal, K. Gopalakrishnan, and P. Narayanan. Deep learning with limited numerical precision. In *Proc. 32nd Int. Conf. Mach. Learn.*, pages 1737–1746, 2015.
- N. J. Higham. *Accuracy and Stability of Numerical Algorithms*. SIAM, Philadelphia, 2002.
- H. Karimi, J. Nutini, and M. Schmidt. Linear convergence of gradient and proximal-gradient methods under the Polyak-Lojasiewicz condition. In *Proc. Jt. Eur. Conf. Mach. Learn. Knowl. Discovery in Databases*, pages 795–811. Springer, 2016.
- S. Linnainmaa. Taylor expansion of the accumulated rounding error. *BIT Numer. Math.*, 16(2):146–160, 1976.
- C. Liu, L. Zhu, and M. Belkin. Loss landscapes and optimization in over-parameterized non-linear int. and neural networks. *Appl. Comput. Harmon. Anal.*, 2022.

- S. Lojasiewicz. A topological property of real analytic subsets. *Coll. du CNRS, Les équations aux dérivées partielles*, 117:87–89, 1963.
- E. Moulay, V. Léchappé, and F. Plestan. Properties of the sign gradient descent algorithms. *Inf. Sci.*, 492: 29–39, 2019.
- T. Na, J. H. Ko, J. Kung, and S. Mukhopadhyay. On-chip training of recurrent neural networks with limited numerical precision. In *Proc. Int. Jt. Conf. Neural Netw.*, pages 3716–3723. IEEE, 2017.
- Y. Nesterov. *Introductory Lectures on Convex Optimization: A Basic Course*. Springer, 2003.
- Q. N. Nguyen and M. Mondelli. Global convergence of deep networks with one wide layer followed by pyramidal topology. In *Proc. 34th Conf. Neural Inf. Process. Syst.*, pages 11961–11972, 2020.
- E. L. Oberstar. Fixed-point representation & fractional math. *Oberstar Consulting*, 9, 2007.
- M. Ortiz, A. Cristal, E. Ayguadé, and M. Casas. Low-precision floating-point schemes for neural network training. *arXiv preprint: 1804.05267*, 2018.
- B. T. Polyak. Gradient methods for solving equations and inequalities. *USSR Comput. Math. & Math. Phys.*, 4(6):17–32, 1963.
- B. T. Polyak. Some methods of speeding up the convergence of iteration methods. *USSR Comput. Math. & Math. Phys.*, 4(5):1–17, 1964.
- M. R. Santoro, G. Bewick, and M. A. Horowitz. Rounding algorithms for IEEE multipliers. In *Proc. 9th Symp. Comput. Arithmetic*, pages 176–183. IEEE, 1989.
- R. Steyer and W. Nagel. *Probability and Conditional Expectation: Fundamentals for the Empirical Sciences*. John Wiley & Sons, 2017.
- N. Wang, J. Choi, D. Brand, C.-Y. Chen, and K. Gopalakrishnan. Training deep neural networks with 8-bit floating point numbers. In *Proc. 32nd Conf. Neural Inf. Process. Syst.*, pages 7675–7684, 2018.
- L. Xia, S. Massei, M. E. Hochstenbach, and B. Koren. On the influence of stochastic roundoff errors on the convergence of the gradient descent method with low-precision floating-point computation. *arXiv preprint: 2202.12276*, 2022.
- R. Yates. Fixed-point arithmetic: An introduction. *Digital Signal Labs*, 81(83):198, 2009.